People's Democratic Republic of Algeria
Ministry of Higher Education and Scientific Research
University Amar Telidji – Laghouat
Department of Mechanical Engineering

Thesis for obtaining the diploma: **Master**
Mechanical Engineering
Option: **Energy**

Presented by:

Boukhalkhal Yacine and Britel Mustapha Ahmed Amine

Thesis :

Validation of Ansys-Fluent Numerical Schemes : Case of Sod Shock Tube

Defended in front of the jury composed of:

Mr. Mohamed Teggar	PR	President	University of Laghouat
Mr. Lakhdar Hachani	PR	Reviewer	University of Laghouat
Mr. Khaled Bensayeh	MCA	Supervisor	University of Laghouat

Graduating Class
June 2024

ملخص

ملخص الدراسة يركز على المحاكاة العددية للموجات الصدمية؛ بالتحديد في سياق مشكلة صدمة سود. تقوم الدراسة بمقارنة دقة وكفاءة الحساب الحاسوبي لـ Ansys fluent ونظام WENO 5 في محاكاة تدفقات الصدمات. تشير النتائج إلى أن نظام WENO تفوق على Ansys fluent من حيث الدقة والكفاءة الحسابية، حيث يتطلب عددًا أقل من العقد الشبكية ووقت حساب أقل لتحقيق نتائج دقيقة. تؤكد الدراسة على أهمية تحسين تقنيات المحاكاة العددية في ديناميات السوائل الحاسوبية لتعزيز فهمنا لسلوك الموجات الصدمية.

Abstract

Summary the study focuses on numerical simulation of shock waves ; particulation in the context of the sod shock problem . it compares the accuracy and computational efficiency of Ansys fluent and a WENO 5 scheme in simulating shock flowes . the results indicate that the WENO scheme outperformed Ansys fluent in terms of accuracy and computational efficiency , requiring fewer mesh nodes and less computation time to achieve precise results . the study emphasizes the importance of improving numerical simulation techniques in computational fluid dynamics to enhance our understanding of shock waves behavior.

Résume

Le résumé de l'étude se concentre sur la simulation numérique des ondes de choc, en particulier dans le contexte du problème de choc de Sod. Il compare la précision et l'efficacité computationnelle de Fluent d'Ansys et d'un schéma WENO 5 dans la simulation des écoulements de choc. Les résultats indiquent que le schéma WENO surpasse Fluent d'Ansys en termes de précision et d'efficacité computationnelle, nécessitant moins de nœuds de maillage et moins de temps de calcul pour obtenir des résultats précis. L'étude met en avant l'importance d'améliorer les techniques de simulation numérique en dynamique des fluides computationnelle pour améliorer notre compréhension du comportement des ondes de choc.

Acknowledgements

ALLAH is the first and the last to be thanked.

First and foremost, I express my sincere gratitude to my supervisor, Associate Professor Khaled Bensayeh , This is for his continuous support during my studies I appreciate his patience, motivation, and extensive knowledge. I am especially thankful for his unwavering support, which provided a clear sense of direction for my research work.

I convey sincere thanks to the committee members: Professor Lakhdar Hachani , Professor Mohamed Teggar

Finally, I extend my sincere thanks to my parents, who are The reason Im here today.

I thank all my family, friends, and those who contributed to this work

Dedication

There is nothing greater than the mercy of the Lord of the universe, who has not withheld His blessings from me. To Him be thanks and praise, abundant praise without end.

To the dearest hearts in my life... my beloved parents.

To the wellspring of tenderness that once burst forth to inspire me with patience and perseverance, to the one who endured until she became today a beacon of knowledge and light, my dear mother.

To my dear father, who endured difficulties and conquered impossibilities for my sake.

To them both, I dedicate this humble work, to bring a little happiness to their hearts. To my brothers and sisters who shared the burdens of life with me.

To my wonderful companions on the journey, I dedicate this research; to thank them for being in my life, for their constant encouragement and pushing me forward, especially in those moments when I was on the verge of despair and surrender.

Britel Mustapha Ahmed Amine

Dedication

I want to express my deep gratitude and heartfelt thanks to my wonderful family, my loyal friends, and my dear professors. With your continuous support and encouragement, I have reached this important day in my life. You have been a strong pillar and a source of inspiration for me at every step of my academic journey. Words of thanks are not enough to express the extent of my gratitude to you and what you have done for me. I hope to always live up to your expectations and continue to make you proud. Thank you from the bottom of my heart.

Boukhalkhal Yacine

Contents

Chapter 03 :Results and Discussion

Liste of figures

Abbreviations and nomenclatures

CFD : Computational Fluid Dynamics

FV : Finite volume

FD : Finite difference

WENO : Weighted Essentially Non-Oscillatory

ENO : Essentially Non-Oscillatory

ρ : Density

u : Velocity

E : Energy

p : Pressure

γ : Ratio of heat capacities

r : Ideal gas constant

T : Temperature

Subscripts

L : Left

R : Right

General Introduction

INTRODUCTION

A shock wave, characterized by a thin layer with abrupt changes in pressure, density, temperature, and other physical properties, can be generated through various mechanisms. These include aerodynamic flow compression in supersonic aircraft or shock tubes, and chemical reactions leading to flow acceleration, known as detonation waves.

Shock waves possess a dual nature, presenting both advantageous and detrimental characteristics depending on the context. In the realm of supersonic aircraft, for instance, shock waves interacting with boundary layers can induce significant heating, potentially inflicting structural harm on the aircraft, as highlighted by [1]. Similarly, uncontrolled detonation waves have been associated with human casualties and material destruction, as reported [2]. These examples underscore the critical importance of comprehending and effectively managing shock waves to mitigate their adverse effects while harnessing their beneficial aspects.

While shock waves can have detrimental effects in certain situations, they also have beneficial applications across industrial and medical domains. [3] Provides a comprehensive examination of the industrial uses of shock waves. Similarly, [4]discusses recent and potential future medical and biomedical applications of shock waves. Furthermore, the detonation wave serves as the foundation for continuous detonation engines, an area of active research that is anticipated to yield significant advancements in aerospace propulsion [5]. Therefore, the study of shock and detonation waves is crucial, as it enables both the mitigation of their undesirable effects and the enhancement of their practical applications.

The accurate simulation of fluid flow phenomena plays a crucial role in numerous engineering applications, ranging from aerospace and automotive design to energy systems and environmental studies. Computational Fluid Dynamics (CFD) has emerged as a powerful tool for the prediction and analysis of fluid flow behavior. Within the realm of CFD, various numerical schemes and solvers have been developed to solve the governing equations of fluid dynamics.

The Sod shock tube is a classic test case widely used in the field of compressible flow simulations. It involves the rapid and highly non-linear transition of gas properties, leading to the formation of shocks and contact discontinuities. The accurate representation of these flow features is essential for understanding the dynamic behavior of compressible flows and optimizing the design of engineering systems.

In recent years, the quest for higher accuracy and improved resolution has led to the development of high-order numerical schemes. These schemes offer several advantages over traditional low-order schemes, such as reduced numerical dissipation and improved capturing of flow discontinuities. One such high-order scheme is the Weighted Essentially Non-Oscillatory (WENO) scheme, which has gained considerable attention due to its ability to accurately resolve shocks and contact discontinuities.

On the other hand, commercial CFD software packages, such as Ansys Fluent, have proven to be valuable tools for solving complex fluid flow problems. These software packages employ various numerical schemes to discretize the governing equations, and they provide a wide range of options to model and simulate different flow phenomena. However, the performance and accuracy of these schemes in capturing flow discontinuities, particularly shocks and contact discontinuities in the context of the Sod shock tube, need to be thoroughly investigated and validated against exact data or high-order schemes like WENO.

The motivation behind this study is to evaluate and compare the performance of the numerical schemes implemented in Ansys Fluent in detecting shocks and contact discontinuities in the context of the Sod shock tube. By comparing the results obtained from Ansys Fluent schemes against exact data and a high-order WENO 5 scheme, we aim to assess the capability of Ansys Fluent in accurately capturing these flow features specific to the Sod shock tube. This evaluation is crucial for understanding the limitations and strengths of Ansys Fluent in simulating compressible flows in the context of this important test case, providing insights into the accuracy and reliability of its numerical schemes.

Furthermore, the findings of this study can help researchers and engineers working on Sod shock tube simulations make informed decisions regarding the choice of numerical schemes for their specific applications. By identifying the strengths and weaknesses of different schemes, they can select the most appropriate scheme for accurately simulating the Sod shock tube and other flow phenomena involving shocks and contact discontinuities.

Overall, this study contributes to the advancement of numerical simulation techniques in CFD and enhances our understanding of the capabilities of Ansys Fluent in predicting and analyzing compressible flows with complex flow features, specifically in the context of the Sod shock tube.

Chapter 01 : Fundamentals sod shock tube

I.1. Introduction:

Shock waves are fascinating physical phenomena that propagate in a variety of mediums, whether in air, water, or even in solid materials. This phenomenon is characterized by a unique set of properties that reflect strong and complex interactions between energy and matter. In this introduction, we will review the definition and characteristics of shock waves, along with their different types and the basics of shock tube, focusing on diaphragm dynamics.

I.2. Definition and Characteristics of Shock Waves:

Explanation of Shock Waves: Shock waves are rapid changes in pressure, temperature and density that propagate through a medium. They are characterized by a sharp increase in pressure followed by a gradual decrease back to equilibrium levels. These waves carry energy and can produce significant effects on the surrounding environment [6]

I.3. Types of Shock Waves:

I.3.1. Normal Shocks: These occur when the flow encounters a sudden decrease in area, causing the flow velocity to exceed the speed of sound locally. Normal shocks are perpendicular to the flow direction.

Examples:

- Supersonic Aircraft.
- Rocket Nozzles.
- Wind Tunnels.
- Supersonic Flow Over Obstacles.

I.3.2. Oblique Shocks: Oblique shocks occur when the flow encounters a change in flow direction. Unlike normal shocks, they are inclined at an angle to the flow direction.

Examples:

- Supersonic Airfoil
- Supersonic Inlets
- Supersonic Flow Around Bodies
- Converging-Diverging Nozzles

I.3.3.Detonation Waves: Detonation waves are highly supersonic shock waves that occur in the process of chemical explosions. They propagate through reactive media such as explosives at speeds faster than the speed of sound in the undisturbed medium.

Examples:

- Highly Supersonic Shock Waves.
- Chemical Explosions.
- Reactive Media.
- Shock Fronts.

I.4. Shock Tube Basics:

I.4.1. Components of a Shock Tube:

- **Driver Section:** This section contains high-pressure gas, typically separated from the driven section by a diaphragm. The driver gas is responsible for generating the shock wave.
- **Driven Section:** The region where the shock wave propagates and interacts with the test medium. It usually contains low-pressure gas or a vacuum to facilitate shock wave propagation.
- **Diaphragm:** A thin membrane separating the driver and driven sections. It ruptures upon triggering, allowing the high-pressure gas from the driver section to expand rapidly into the driven section, generating a shock wave.
- **Test Section:** This is where experiments are conducted to study the effects of shock waves on various materials or structures. It's the area where researchers observe and measure the behavior of the shock wave [7].

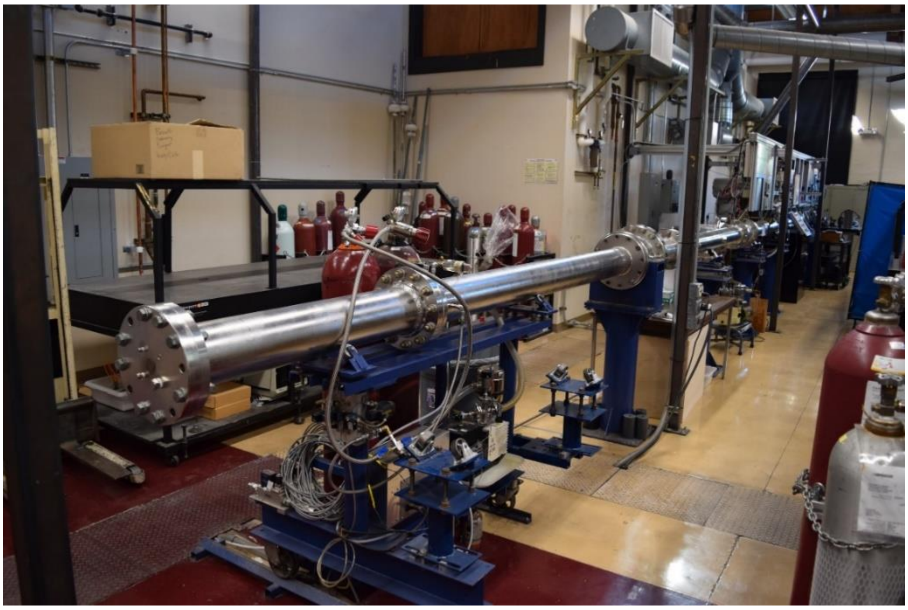

Figure 1. Image release for the sod shock tube, Stanford University.

I.5. Working Principle:

The shock tube operates based on the sudden release of high-pressure gas from the driver section into the driven section.

When the diaphragm ruptures, the high-pressure gas rapidly expands into the low-pressure driven section, generating a shock wave in the process.

The shock wave then travels through the driven section, interacting with the test medium in the test section where experiments are conducted to study the characteristics and effects of the shock wave [8].

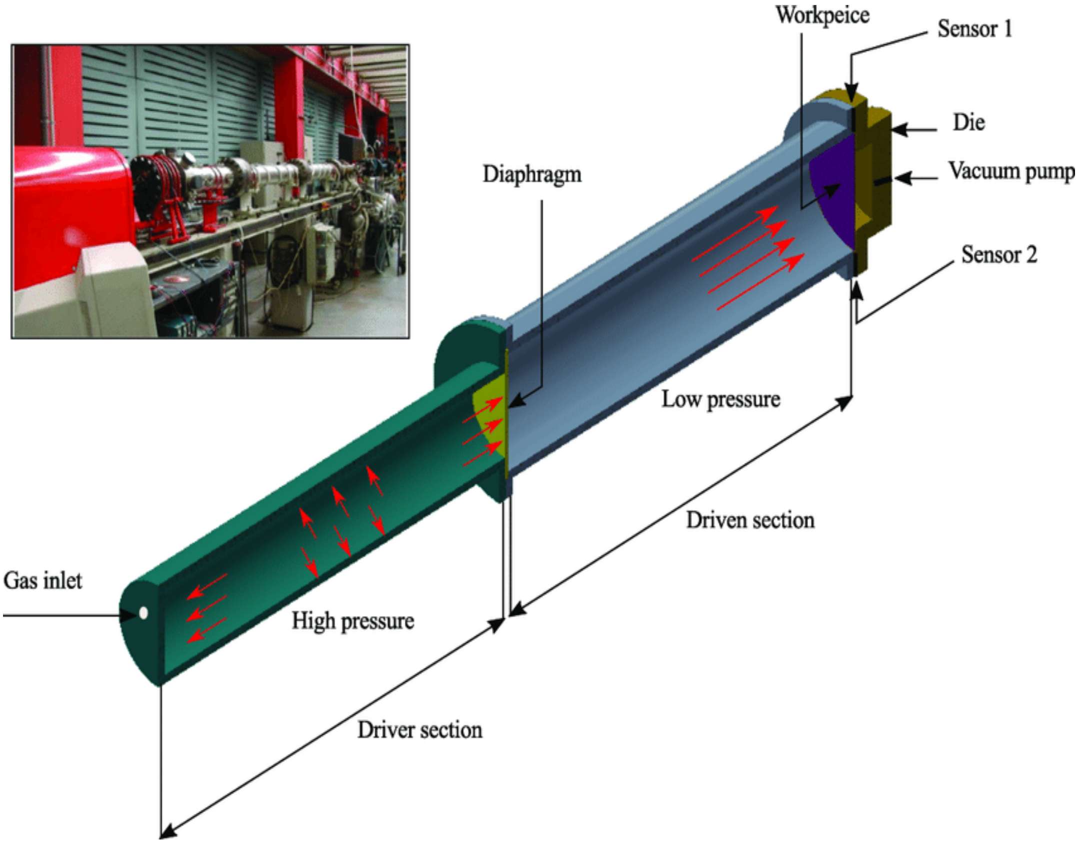

Figure 2. A schematic representation the experimental setup of the shock wave tube forming process. Inset: The shock tube facility at the Institute of General Mechanics, RWTH Aachen University.

I.6. Tube Geometries and Configurations:

I.6.1. Types of Pipes:

- Straight Tube.
- Reflected Shock Tube.
- Expansion Tube.
- Shock Tunnel [9].

I.7. Diaphragm Dynamics:

I.7.1. Role of Diaphragm Rupture in Generating Shock Waves:

The diaphragm plays a crucial role in shock tube operation by separating the high-pressure driver section from the low-pressure driven section.

Upon rupture, it allows the rapid expansion of high-pressure gas into the driven section, generating a shock wave [10]

I.7.2. Materials and Design Considerations:

Diaphragms are typically made from thin membranes of materials such as Mylar, Kapton, or aluminum.

Design considerations include material strength, thickness and flexibility to ensure reliable and controlled rupture under specified conditions.

I.7.3. Instrumentation and Measurement Techniques:

- Pressure Transducers, High-speed Cameras, and Schlieren Photography
- Measurement of Shock Wave Parameters: Pressure, Temperature, and Velocity

I.8. Scope of the present work:

The aim of this study is to utilize computational methods for accurately modeling and simulating the dynamic behavior of shock tubes. By developing advanced numerical techniques and models, we aim to achieve the following objectives:

1- Enhancing our understanding of the propagation, reflection and interaction of shock waves with obstacles.
2- Uncovering the fundamental mechanisms that govern the behavior of shock tubes.
3- Verifying computed results against experimental data.
4- Facilitating the interpretation of experimental results. [11].

Chapter 02 : Numerical Solution

Chapter 02:
Numerical Solution

II.1. Introduction:

The Sod's one-dimensional shock tube problem stands as a cornerstone in Riemann problems. Essentially, it involves a virtual diaphragm within a shock tube, segregating the fluid into distinct states characterized by varying density, velocity and pressure. When time t=0 strikes, this virtual diaphragm swiftly retreats, triggering an array of waves—be it shock, rarefaction, or contact discontinuity—rippling through the fluid field, thereby altering its state distribution.

This particular problem wields a unique prowess in scrutinizing the stability and resolution of numerical schemes. Its efficacy lies in the simplicity of the control equation, boasting fewer dimensions and variables, yet encapsulating a spectrum of CFD discontinuities. Tackling these discontinuous phenomena has perennially posed a challenge and remained a pivotal concern in CFD advancement, lending profound significance to numerical simulations.

The Riemann problem offers an exact solution, furnishing a litmus test for the accuracy of numerical methods. In this study we employ fifth-order WENO To compare with the Ansys fluent.

II.2. Governing Equations:

In addition to the Navier-Stokes equations, shock tube simulations often require specialized equations to accurately represent the dynamics of shock waves. Among these are the Euler equations, which omit viscosity effects and are particularly suited for high-speed, compressible flows characteristic of shock wave phenomena. Furthermore, the inclusion of an energy equation enables the modeling of thermal effects and energy transport, enhancing the fidelity of simulations in capturing shock wave behavior.

II.2.1. Discontinuity Distribution:

At t=0, the velocity inside the tube is zero, and the high-pressure zone is to the left of the diaphragm. When the diaphragm is removed, the initial pressure difference will propagate to the right as a shock wave, while an isentropic rarefaction wave will propagate to the left. [12] [13]

II One-dimensional Euler Equations

Consider the conserved form of Euler equations for one-dimensional unsteady flow without considering the heat source, heat conduction and volume forces:

$$\frac{\partial \rho}{\partial t} + \frac{\partial(\rho u)}{\partial x} = 0 \qquad (1)$$

$$\frac{\partial(\rho u)}{\partial t} + \frac{\partial(\rho u^2 + p)}{\partial x} = 0 \qquad (2)$$

$$\frac{\partial E}{\partial t} + \frac{\partial(u(E+p))}{\partial x} = 0 \qquad (3)$$

Where E is the energy per unit volume (length).

One more equation to close the system:

$$E = \frac{1}{\gamma - 1}\frac{p}{\rho} + \frac{1}{2}u^2 \qquad (4)$$

For describing one-dimensional flow problems, the conservation form of the inviscid Euler equations can be written in Cartesian space co-ordinates system as follows:

$$\frac{\partial U}{\partial t} + \frac{\partial f(U)}{\partial x} = 0 \qquad (5)$$

Denote:

$$\begin{aligned} U &= [\rho, \rho u, \rho E]^T \\ f(U) &= [\rho u, \rho u^2 + p, (\rho E + p)u]^T \end{aligned} \qquad (6)$$

Here, vector U is the solution vector of conserved variables and vector F is the inviscid flux vector, ρ denotes the density, u represent velocity component in the x Cartesian direction.

We denote the pressure by P, the total internal energy per unit mass by E, and
The ideal gas equation of state is assumed the pressure relating the E as:

$$P = (\gamma - 1)\rho\left[E - \frac{u^2}{2}\right] \qquad (7)$$

Where γ is the specific heat ratio, equation (5) can be written in characteristic mode.

$$\frac{\partial U}{\partial t} + A\frac{\partial U}{\partial x} = 0 \qquad (8)$$

With:

$$A = \frac{\partial f}{\partial U} = \begin{bmatrix} 0 & 1 & 0 \\ \frac{-(3-\gamma)u^2}{2} & (3-\gamma)u & \gamma - 1 \\ \frac{(\gamma-2)u^3}{2} - \frac{uc^2}{\gamma-1} & \frac{c^2}{\gamma-1} + \frac{(3-2\gamma)u^2}{2} & \gamma u \end{bmatrix}$$

Where c is the acoustic velocity, which can be given as:

$$c^2 = \frac{\gamma p}{\rho}$$

The matrix A can be diagonalized:

$$A = S^{-1}AS$$

where Λ is the Diagonal matrix, S the transformational matrix.

The eigenvalues of matrix A are:

$$\lambda_1 = u, \lambda_2 = u - c, \lambda_3 = u + c$$

II.3. Numerical Methods:

II.3.1. High Resolution Schemes:

To obtain a numerical approximation of the Euler equations, there is a several numerical schemes to determine which is the most accurate. All these schemes are high resolution schemes, i.e. they are second order accurate away from shocks and satisfy the Total Variational Diminishing (TVD) property. One of these schemes is based on Roe's scheme [14] and was discussed by Hubbard & Garcia-Navarro [15] , the other scheme is the HLLE scheme [16] [17] [18]

The Euler equations are a system of homogeneous conservation laws

$$\mathbf{U}_t + \mathbf{F}(\mathbf{U})_x = 0$$

where $\mathbf{F}(\mathbf{U})$ is the flux-function. To obtain a conservative approximation of homogeneous systems of conservation laws, we only consider numerical schemes of the form

$$\mathbf{U}_i^{n+1} = \mathbf{U}_i^n - s\left(\mathbf{F}^*_{i+\frac{1}{2}} - \mathbf{F}^*_{i-\frac{1}{2}}\right)$$

where $s = \frac{\Delta t}{\Delta x}$, Δx and Δt are the step sizes in space and time respectively, $\mathbf{F}^*_{i+\frac{1}{2}}$ is the numerical flux and

$$\mathbf{U}_i^n \approx \frac{1}{\Delta x}\int_{x_{i-\frac{1}{2}}}^{x_{i+\frac{1}{2}}} \mathbf{U}(x, t^n)dx$$

is the numerical approximation.

To ensure the schemes remains stable, the time step is calculated using

$$\Delta \mathrm{t} = \frac{\nu \Delta \mathrm{x}}{\max(|\lambda|)}$$

where $\max(|\lambda|)$ is the maximum wave speed and $\nu \leq 1$ is the required Courant (CFL) number.

We now present a discussion and discretisation of the three schemes

II.3.2. Roe's scheme:

Hubbard & Garcia-Navarro [19] discussed an adapted form of Roe's scheme [20] which is a high-resolution scheme. The numerical flux-function is

$$\mathrm{F}^*_{\mathrm{i}+\frac{1}{2}} = \frac{1}{2}(\mathrm{F}^n_{\mathrm{i}+1} + \mathrm{F}^n_{\mathrm{i}}) - \frac{1}{2}\sum_{k=1}^{p}\left[\tilde{\alpha}_k|\tilde{\lambda}_k|\big(1 - \Phi(\theta_k)(1 - |\nu_k|)\big)\tilde{e}_k\right]_{\mathrm{i}+\frac{1}{2}}$$

where

$$\nu_k = s\tilde{\lambda}_k,\ \theta_k = \frac{(\tilde{\alpha}_k)_{\mathrm{I}+\frac{1}{2}}}{(\tilde{\alpha}_k)_{\mathrm{i}+\frac{1}{2}}},\ \mathrm{I} = \mathrm{i} - \mathrm{sgn}(\nu_k)_{\mathrm{i}+\frac{1}{2}}$$

and $\Phi(\theta_k)$ is the minmod flux-limiter,

$$\Phi(\theta_k) = \max\big(0, \min(1, \theta_k)\big)$$

Here, the $\sim$ is called the Roe average and $\tilde{\lambda}$, $\tilde{e}$ and $\tilde{\alpha}$ are the eigenvalues, eigenvectors and wave strengths of the Roe averaged Jacobian matrix, $\tilde{A}$. The Roe averaged eigenvalues, eigenvectors and wave strengths are determined from the Roe decomposition (see [21,22,23] for more details)

$$\Delta F = \sum_{k=1}^{p} \tilde{\alpha}_k \tilde{\lambda}_k \tilde{e}_k = \tilde{A}\Delta U$$

where $\Delta U = U_R - U_L$ and p is the number of components in the system ($p = 3$ for the Euler equations).

For the Euler equations with ideal gases, Toro [21] obtained the following Roe averaged Jacobian matrix,

$$\tilde{A} = \begin{bmatrix} 0 & 1 & 0 \\ \frac{1}{2}(\gamma-3)\tilde{u}^2 & (3-\gamma)\tilde{u} & \gamma-1 \\ \tilde{u}\left(\frac{1}{2}(\gamma-1)\tilde{u}^2 - \tilde{H}\right) & \tilde{H}-(\gamma-1)\tilde{u}^2 & \gamma\tilde{u} \end{bmatrix}$$

whose eigenvalues are

$$\tilde{\lambda}_1 = \tilde{u} - \tilde{a},\ \tilde{\lambda}_2 = \tilde{u} \ \text{ and } \ \tilde{\lambda}_3 = \tilde{u} + \tilde{a}$$

with corresponding eigenvectors

$$\tilde{e}_1 = \begin{bmatrix} 1 \\ \tilde{u}-\tilde{a} \\ \tilde{H}-\tilde{u}\tilde{a} \end{bmatrix},\ \tilde{e}_2 = \begin{bmatrix} 1 \\ \tilde{u} \\ \frac{1}{2}\tilde{u}^2 \end{bmatrix} \ \text{ and } \ \tilde{e}_3 = \begin{bmatrix} 1 \\ \tilde{u}+\tilde{a} \\ \tilde{H}+\tilde{u}\tilde{a} \end{bmatrix}$$

where the Roe average values are

$$\tilde{u} = \frac{\sqrt{\rho_L}u_L + \sqrt{\rho_R}u_R}{\sqrt{\rho_L}+\sqrt{\rho_R}},\ \tilde{H} = \frac{\sqrt{\rho_L}H_L + \sqrt{\rho_R}H_R}{\sqrt{\rho_L}+\sqrt{\rho_R}}$$

And

$$\tilde{a} = \sqrt{(\gamma-1)\left(\tilde{H} - \frac{1}{2}\tilde{u}^2\right)}$$

Toro also determined the following wave strengths,

$$\tilde{\alpha}_2 = \frac{(\gamma-1)}{\tilde{a}^2}\left(\left(\tilde{H}-\tilde{u}^2\right)\Delta\rho + \tilde{u}\Delta(\rho u) - \Delta E\right)$$

$$\tilde{\alpha}_1 = \frac{1}{2\tilde{a}}\left((\tilde{u}+\tilde{a})\Delta\rho - \Delta(\rho u) - \tilde{a}\tilde{\alpha}_2\right),\ \text{ and } \ \tilde{\alpha}_3 = \Delta\rho - (\tilde{\alpha}_1 + \tilde{\alpha}_2)$$

II.3.2. HLLE scheme :

Einfeldt et al. [22] discussed an adapted version of the HLL scheme [23] called the HLLE scheme, which can be viewed as a modification of Roe's scheme. In this paper, we adapt the HLLE scheme to a high-resolution scheme,

$$F^{*}_{i+\frac{1}{2}} = \frac{1}{2}(F^{n}_{i+1} + F^{n}_{i}) - \frac{1}{2}\sum_{k=1}^{p} \left[\tilde{\alpha}_k \tilde{Q}_k \left(1 - \Phi(\theta_k)\left(1 - s\tilde{Q}_k\right)\right) \tilde{e}_k\right]_{i+\frac{1}{2}},$$

Where:

$$\left(\tilde{Q}_k\right)^{n}_{i+\frac{1}{2}} = \left[\frac{(b^{+} + b^{-})\tilde{\lambda}_k - 2b^{+}b^{-}}{b^{+} - b^{-}}\right]^{n}_{i+\frac{1}{2}},$$

$$b^{+}_{i+\frac{1}{2}} = \max\left(b^{R}_{i+\frac{1}{2}}, 0\right),\ b^{-}_{i+\frac{1}{2}} = \min\left(b^{L}_{i+\frac{1}{2}}, 0\right)$$

and the numerical signal velocities for the Euler equations with ideal gases are

$$b^{R}_{i+\frac{1}{2}} = \max(\tilde{u} + \tilde{a}, u^{n}_{i+1} + a^{n}_{i+1}) \text{ and } b^{L}_{i+\frac{1}{2}} = \min(\tilde{u} - \tilde{a}, u^{n}_{i} - a^{n}_{i})$$

Chapter3: Results and discussion

Chapitre 03 :

Results and Discussion

III.1. Introduction

The Sod shock tube is a Riemann problem used to test the accuracy of computational methods. A shock tube consists of a tube of circular or rectangular cross-section filled with gas. The tube is divided into two parts by a diaphragm placed in its middle (see Figure 3). Numerically, the diaphragm is modeled as a discontinuity in the initial conditions of the fluid (density, pressure, and temperature) across this surface. The shock tube is a widely used tool in the field of computational fluid dynamics (CFD) to test the accuracy and performance of different calculation methods.

Configuration: The shock tube consists of a long tube of circular or rectangular section filled with a gas, usually air or a specific gas mixture. The tube is divided into two sections by a diaphragm or piston positioned in the middle.

Initial conditions: Initially, the gas on both sides of the diaphragm exhibits different properties such as density, pressure, and temperature. These properties are carefully chosen to create a region of high pressure on one side and a region of low pressure on the other, thus establishing the conditions necessary for the formation of a shock wave.

The initial conditions are very simple for this problem: a contact discontinuity separating gases of different pressure and density, and zero velocity everywhere. In the standard case, the density and pressure on the left are both equal to unity. The density on the right side of the membrane is 0.125 and the pressure is 0.1. The ratio of specific heats is 1.4. The initial conditions can be summarized in the following equation.

$$\begin{pmatrix} \rho_L \\ p_L \\ u_L \end{pmatrix} = \begin{pmatrix} 1.0 \\ 1.0 \\ 0.0 \end{pmatrix} \quad , \quad \begin{pmatrix} \rho_R \\ p_R \\ u_R \end{pmatrix} = \begin{pmatrix} 0.125 \\ 0.1 \\ 0.0 \end{pmatrix} \tag{9}$$

A t=0, the diaphragm is instantaneously removed (this is done experimentally using a thin metal sheet, and a small explosion bursts the diaphragm).

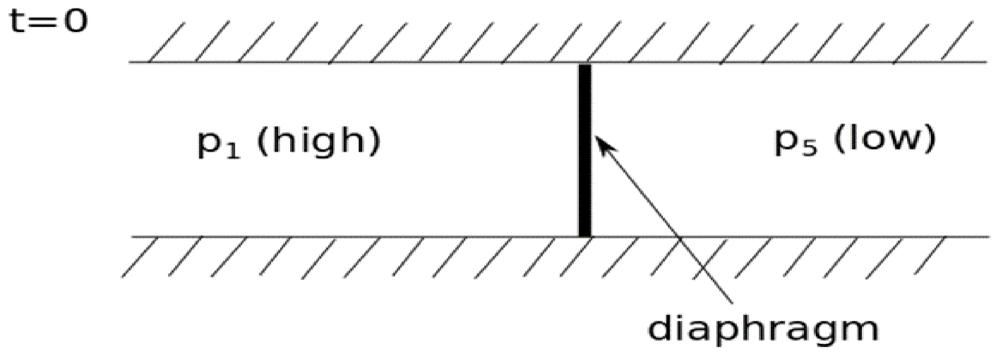

Figure 3. initial state.

III.2. Diaphragm release:

The diaphragm is then abruptly removed or ruptured, allowing the high-pressure gas to rapidly expand towards the low-pressure region. This creates a shock wave that propagates through the tube.

The rupture of the diaphragm causes a 1D unsteady flow consisting of a steadily moving shock - a Riemann problem. A discontinuity is present, and the solution is self-similar with 5 regions.

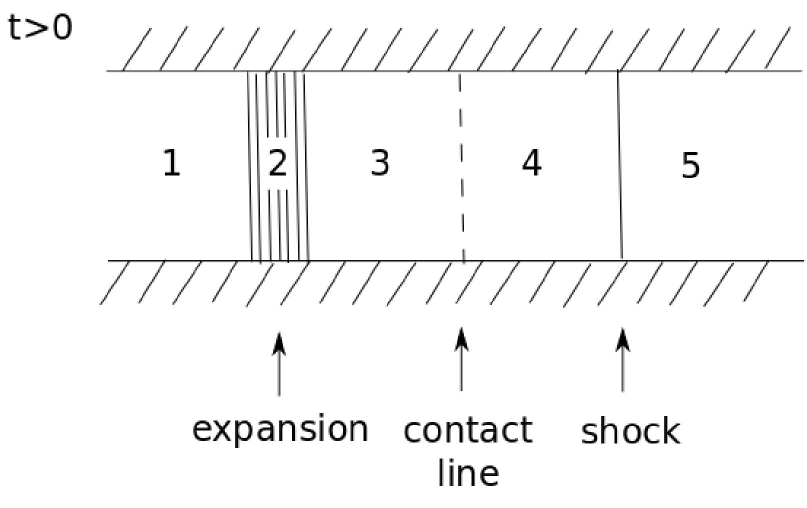

Figure 4. The bursting of the diaphragm .

Shock wave propagation :

As the shock wave travels through the tube, it interacts with the gas and alters its properties such as pressure, density and velocity. The shock wave creates a sharp transition between regions of high pressure and low pressure.

Regions 1 and 5 - left and right sides of the initial states

Region 2 - expansion or rarefaction wave (state dependent on x)

Regions 3 and 4 - stable states independent of x within the region (uniform)

The contact line between regions 3 and 4 separates fluids of different entropy (but they have the same pressure and velocity), meaning it's an invisible line - for example, two fluids, one containing water and the other dye - the contact line moves ($p3=p4$ and $u3=u4$).

computational methods :

Various computational methods such as finite difference, finite volume, or finite element methods are used to simulate the behavior of the shock wave and gas flow in the tube. These methods numerically solve the fundamental equations of fluid dynamics.

Computational and validation: Simulated results obtained from computational methods are compared to experimental measurements or analytical solutions to assess the accuracy and reliability of the numerical algorithms. This allows researchers to validate and refine their models and computational algorithms.

By using the shock tube as a test case, researchers can study the ability of computational methods to accurately capture and predict complex flow phenomena associated with shock waves, including shock wave propagation, reflection, and interaction with obstacles. The shock tube provides a controlled and reproducible experimental setup, making it a valuable tool for evaluating the performance of computational methods in simulating real fluid dynamics problems.

Shock tubes have numerous applications in fluid dynamics research. Here are some common areas where shock tubes are used:

1. Shock wave studies: Shock tubes are widely used to investigate the behavior and characteristics of shock waves. They provide a controlled environment to generate and study shock waves, enabling researchers to investigate phenomena such as shock wave propagation, reflection, diffraction, and interaction with obstacles.

2. Research on hypersonic flows: Shock tubes are valuable tools for studying hypersonic flows, which occur at extremely high speeds. They allow researchers to simulate the conditions encountered by vehicles, such as spacecraft or missiles, during atmospheric re-entry. Shock tubes help understand the aerodynamic forces, heat transfer and flow characteristics associated with hypersonic flight.

3. Supersonic combustion and propulsion: Shock tubes are used to study supersonic combustion processes and evaluate the performance of supersonic combustion engines. They assist researchers in understanding ignition, combustion, and flame propagation in high-speed flows, which is essential for the development of advanced propulsion systems.

4. Turbulence research: Shock tubes can generate turbulent flows, making them useful for studying turbulence characteristics and turbulent mixing. They provide controlled conditions to investigate the behavior of turbulent flows, such as turbulence dissipation, turbulence statistics, and turbulent transport phenomena.

5 Materials science and shock physics: Shock tubes are used in materials science research to study the response of materials to high-pressure and high-temperature conditions. They help researchers investigate the behavior of materials under shock loading, such as shock-induced phase transitions and material strength properties.

6. Verification and validation of numerical models: Shock tubes serve as benchmarks for the validation and verification of numerical models and computational methods. Researchers compare experimental data obtained from shock tube experiments to numerical simulations to assess the accuracy and reliability of their computational fluid dynamics (CFD) codes.

Overall, shock tubes play a crucial role in advancing our understanding of various fluid dynamics phenomena, allowing researchers to develop more accurate numerical models, improve engineering designs, and enhance the performance of systems operating under extreme conditions.

III.3. THE PURPOSE OF THE STUDY:

The main objective of the in-depth study on shock tubes is to compare and diagnose the numerical schemes used by Ansys Fluent with high-fidelity schemes such as WENO 5 schemes. Furthermore, the results obtained from these different methods will also be compared to exact solutions.

By conducting this comparison, researchers seek to evaluate the accuracy and performance of the numerical schemes used in Ansys Fluent compared to high-fidelity schemes such as WENO 5.

Numerical schemes are methods used to discretize the equations of fluid dynamics and numerically solve flow problems. It is crucial to determine the validity and reliability of these schemes, as they have a direct impact on the accuracy of the results obtained.

By comparing the results of Ansys Fluent numerical schemes with high-fidelity schemes such as WENO 5, researchers can identify the strengths and weaknesses of each method. High-fidelity schemes are known for their ability to accurately capture complex flow phenomena, but they can also be more computationally expensive. On the other, numerical schemes used in commercial software like Ansys Fluent are generally faster but may introduce approximations that affect result accuracy.

By comparing the results with exact solutions of the studied problem, researchers can evaluate the ability of different methods to reproduce real results. This allows quantifying the error of each method and determining which one provides results closest to reality.

In summary, the in-depth study of the shock tube aims to compare Ansys Fluent numerical schemes with high-fidelity schemes such as WENO 5 and confront them with exact solutions. This comparison enables the evaluation of the accuracy and performance of different methods, thus providing valuable insights for improving numerical schemes and optimizing fluid dynamics calculations.

III.4. Results and discussion

Geometry:

The tube has a rectangular cross-section with dimensions of 0.1m and a length of 1m. The geometry is presented in Figure 5.

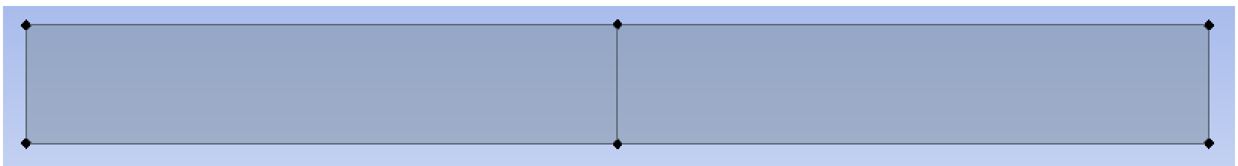

Figure 5. Geometry of the shock tube.

Mesh 1:

The geometry and numerical mesh were created using only the Design Modeler and Mesh tools, which are integral parts of Ansys. The basic mesh generator allows for the creation of quadrilateral meshes in a very simple and fast manner. Since we are considering the 1D case, the mesh in the y-direction contains only one cell. For the x-direction, 100 cells were used.

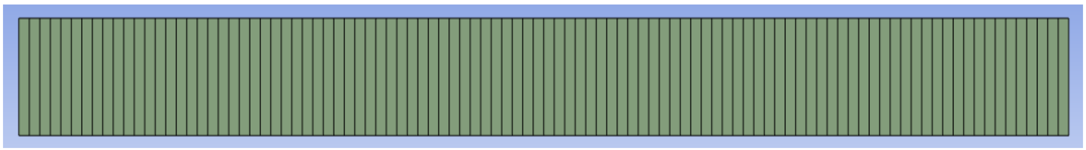

Figure 6. Mesh 1-100 of shock tube.

Solver and boundary conditions:

The Rho solver was used to compute the Sod shock tube problem. It is a transient solver based on density for compressible fluid flow. The working fluid is air, with its thermophysical properties. It is noted that the dynamic viscosity μ is set to 0 (as we aim to solve the Euler equations) and that turbulence modeling is set to laminar. The Prandtl number is not used in this case. We use the ideal gas law as the equation of state.

The inviscid model is used since it involves solving the Euler equations as follows:

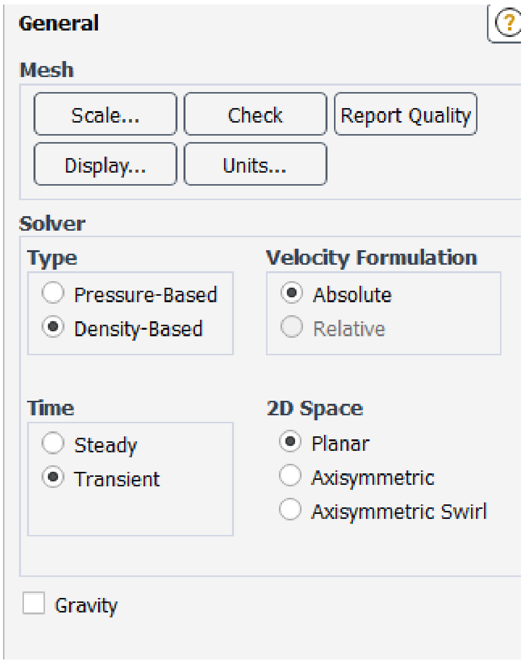

Figure 7. Density-Based solution **.**

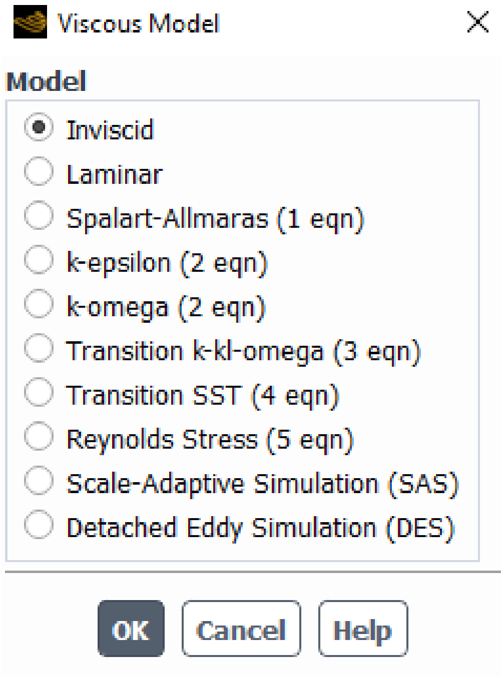

Figure 8. viscous model .

Air is modeled as an ideal gas, and its properties are defined as indicated below:

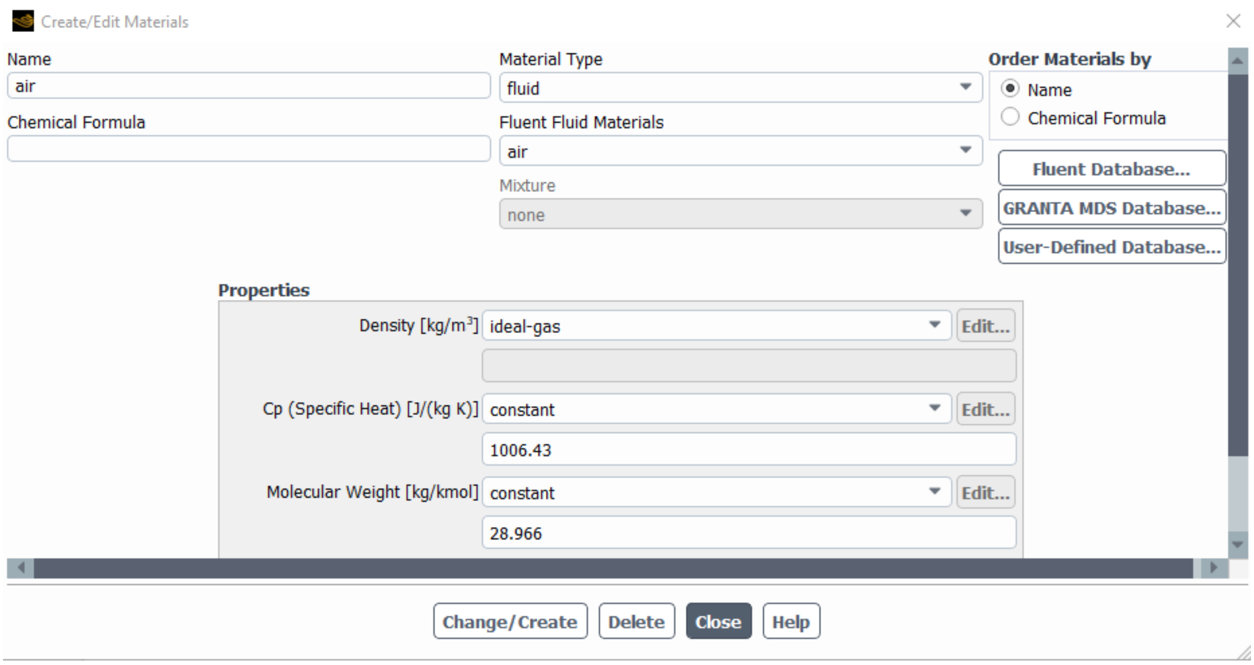

Figure 9. Fluid properties **.**

All boundaries are treated as walls and we apply "zero gradient" conditions for all flow variables because it's a non-viscous flow, as indicated in the following figure.

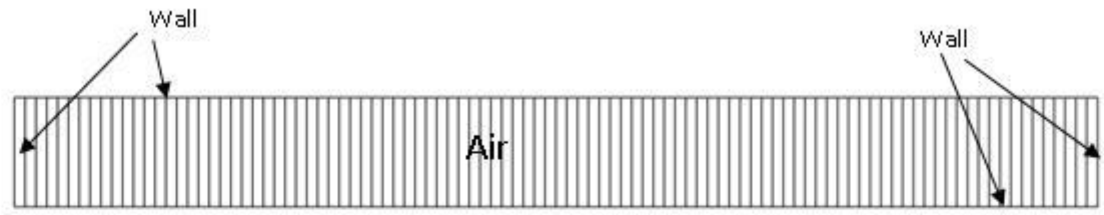

Figure 10. Boundary conditions.

For the solver, the formulation is entirely explicit and the Roe scheme is used for flux decomposition with a number CFL=0.9 <1 is used.

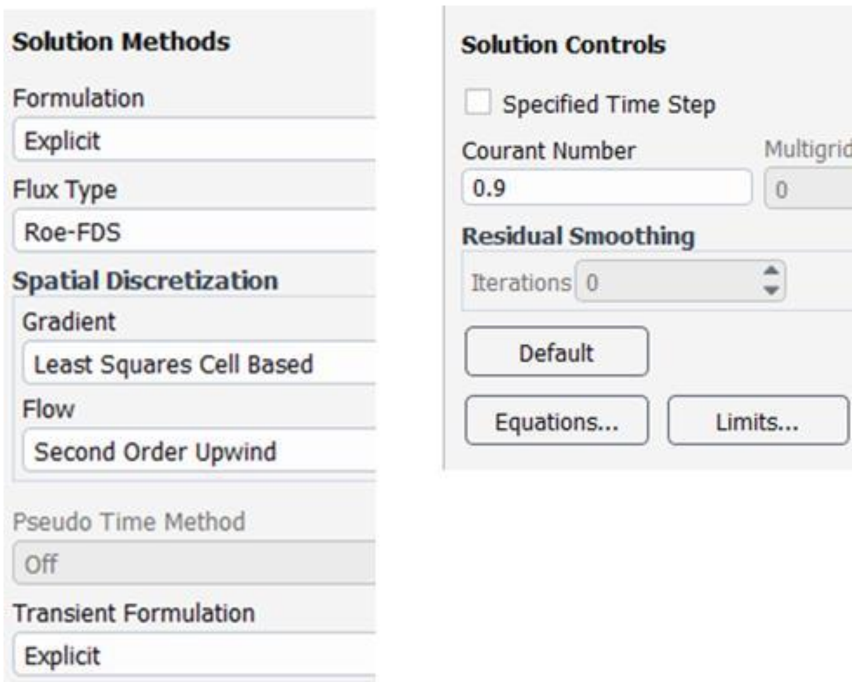

Figure 11. Solution methods and CFL number.

For a proper initialization of the model, we have set the domain at t=0s according to equation (1), defining p, U, and T for the left and right sides of the domain. Since we are dealing with compressible flow with strong discontinuities such as shock waves, robust and accurate numerical schemes must be considered. The method of least squares has been used for gradient schemes and limited linear schemes for convective terms. The momentum and energy equations are discretized using second-order Upwind schemes

The density is initialized according to the equation (1), $\rho=1$ For $x<0.5$ and $\rho=0.125$ For $0.5<x<1.0$ as shown in the following

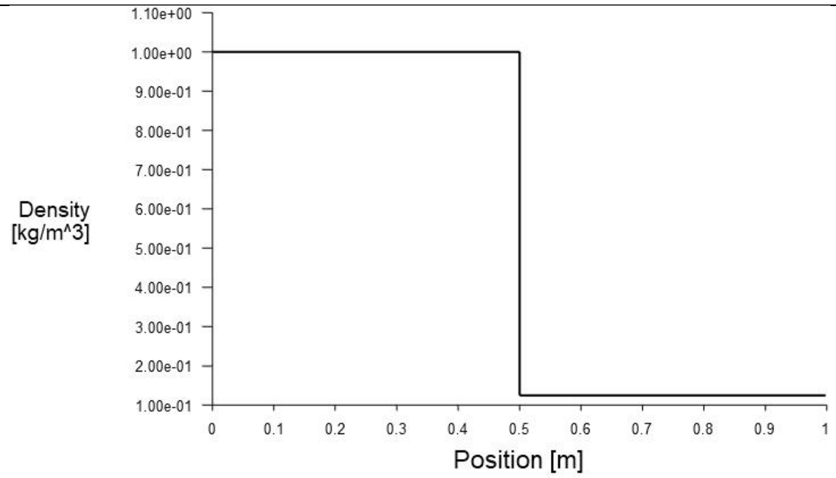

a

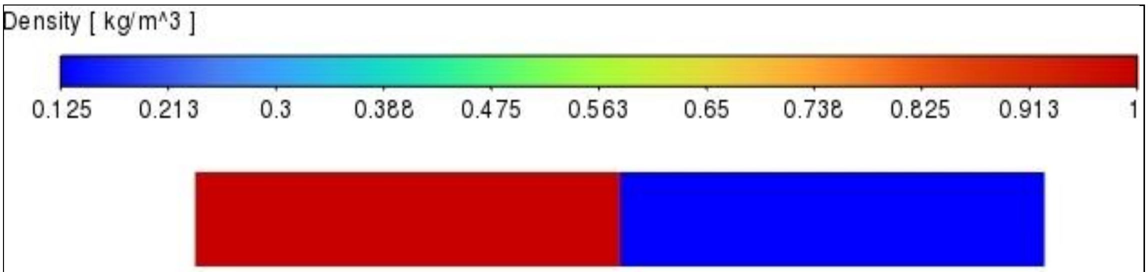

b

Figure 12. Density Initialization a) density distribution on the x axis and b) density contour.

A zero velocity is initialized throughout the entire computational domain , u=0 verser 0.0<u<1.0

a

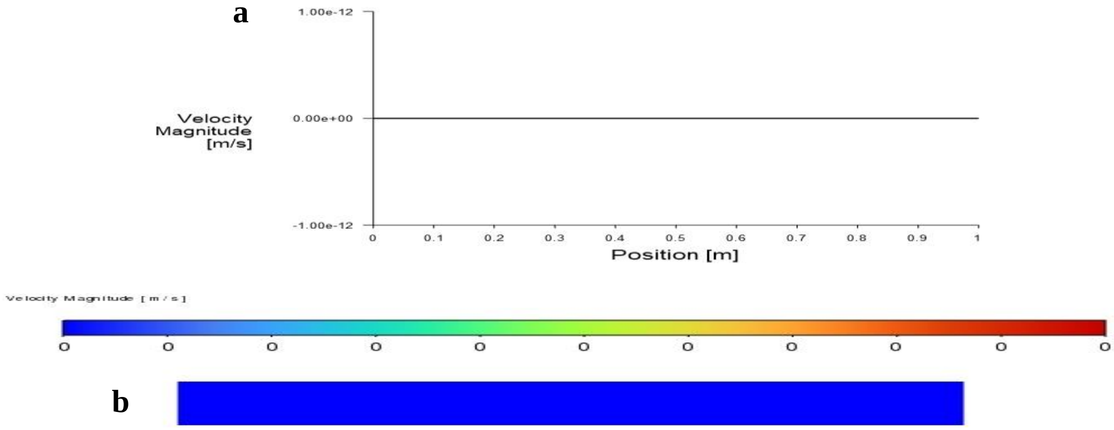

b

Figure 13. Initialization of Velocity a) velocity distribution along the x-axis and b) velocity contour.

III.5. Comparison of numerical schemes for hyperbolic equations

In the field of shock waves and discontinuity capture, the comparison of numerical schemes for solving hyperbolic equations is based on three main criteria:

1.Calculation accuracy:

The numerical scheme must be capable of accurately reproducing the analytical solution of the hyperbolic equation. It is important to avoid Gibbs oscillations, which can introduce significant errors in the results.

2.Computational consumption:

For a given calculation accuracy, it is desirable to choose the numerical scheme that minimizes computational resource consumption. This allows for obtaining solutions more quickly and with lower energy costs.

3.Mesh:

The numerical scheme should be capable of operating with the finest mesh possible. This allows for capturing fine details of the solution and obtaining more accurate results.

In summary, the comparison of numerical schemes for hyperbolic equations is based on compromise between accuracy, computational consumption, and mesh refinement.

The choice of the optimal scheme will depend on the specific requirements of the application.

Examples of numerical schemes

Here are some examples of numerical schemes commonly used for hyperbolic equations:

Lax-Wendroff scheme:

This scheme is simple to implement and offers good computational accuracy. However, it may be subject to Gibbs oscillations.

MacCormack scheme:

This scheme is more accurate than the Lax-Wendroff scheme and is less prone to Gibbs oscillations. However, it is more complex to implement.

Godunov scheme:

This scheme is highly accurate and is capable of capturing discontinuities without Gibbs oscillations. However, it is more complex to implement than the previous schemes.

Conclusion: The choice of the optimal numerical scheme for solving hyperbolic equations depends on the specific application. It's important to consider three main criteria: computational accuracy, computational cost, and mesh.

Resolving real flow with shock scenarios nonetheless presents numerous challenges, some of which are outlined below:

1. Shocks are discontinuous regions of the numerical solution that require special treatment to avoid certain non-physical oscillations known as Gibbs oscillations.

2. Real flow scenarios often exhibit discontinuities and fine structures. However, shock-capturing methods are generally recognized for their dissipative nature. Therefore, it is essential to design shock-capturing schemes that are weakly dissipative to accurately resolve all flow characteristics.

3. Real flows are often turbulent and exhibit shock-turbulence interactions. Therefore, it is interesting to incorporate accurate turbulence models to capture these interactions.

4. Simulating flows with shocks incurs a high numerical cost. Therefore, efforts to reduce computational time, whether through parallel computing or optimization of numerical methods, are of great interest.

Mesh results 1-100

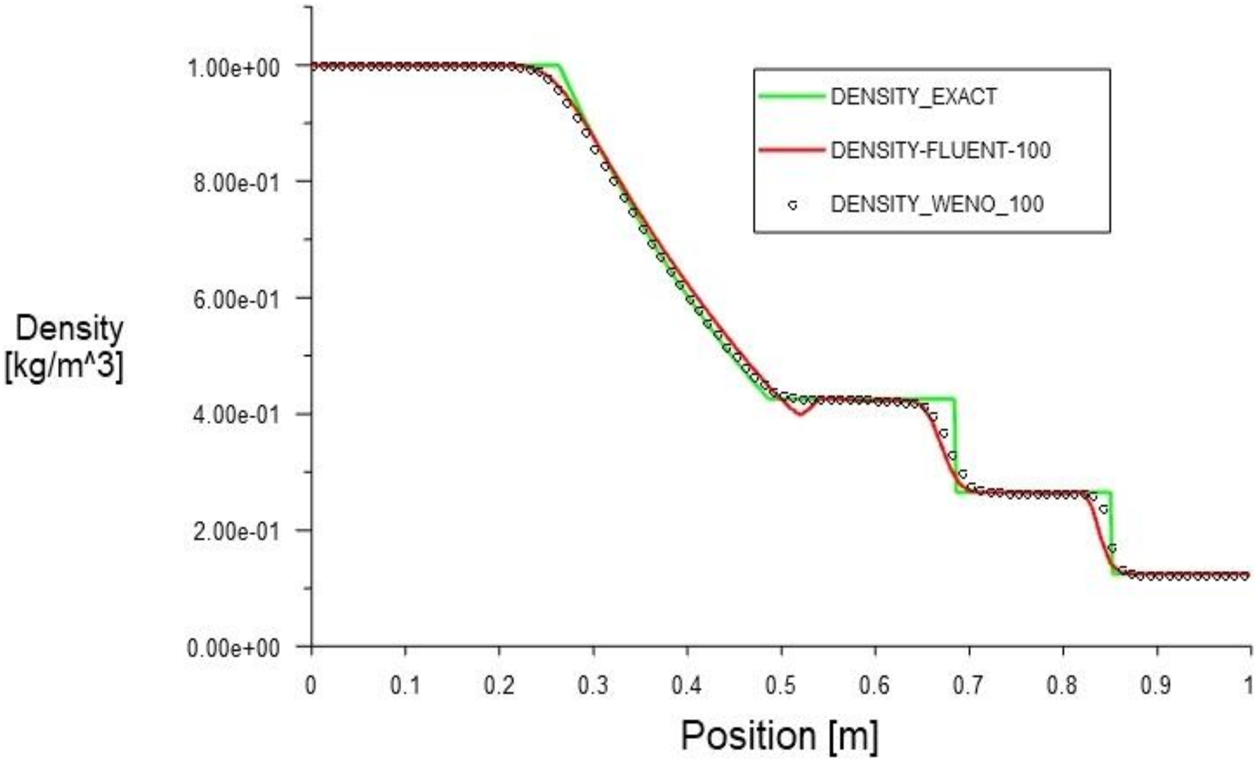

Figure 14. Variation of density along the shock tube.

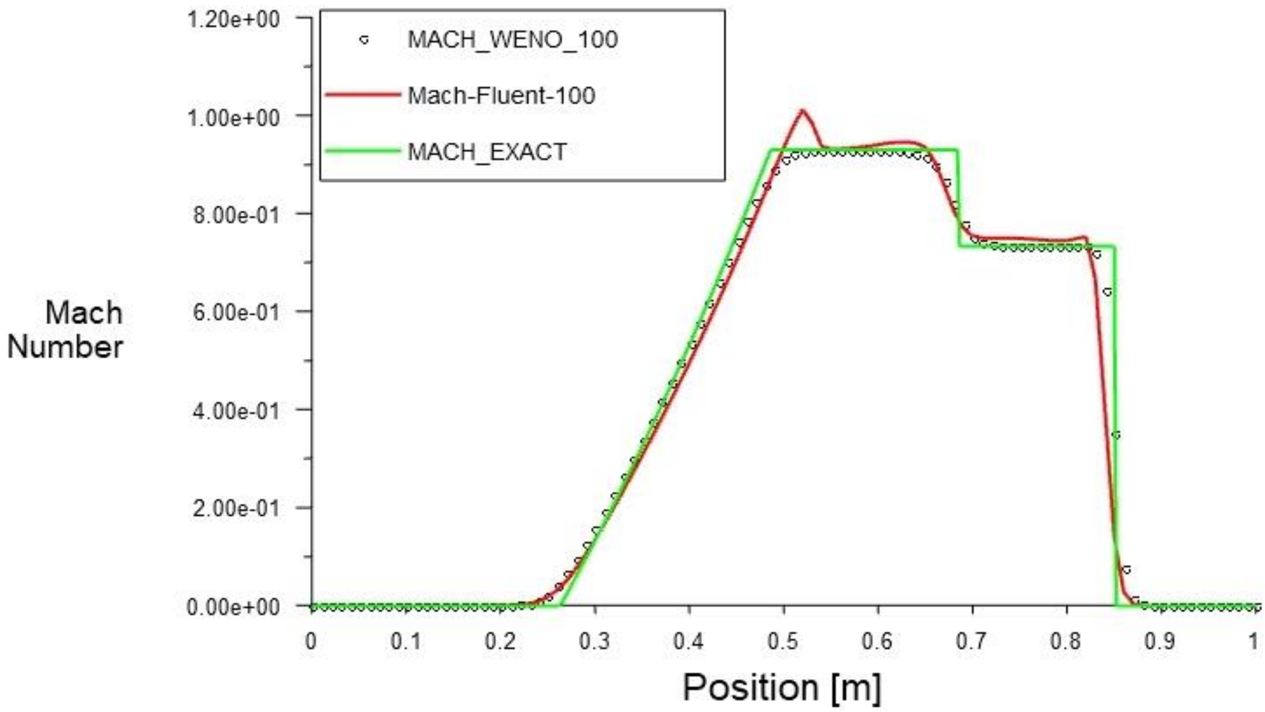

Figure 15. Variation of Mach along the shock tube.

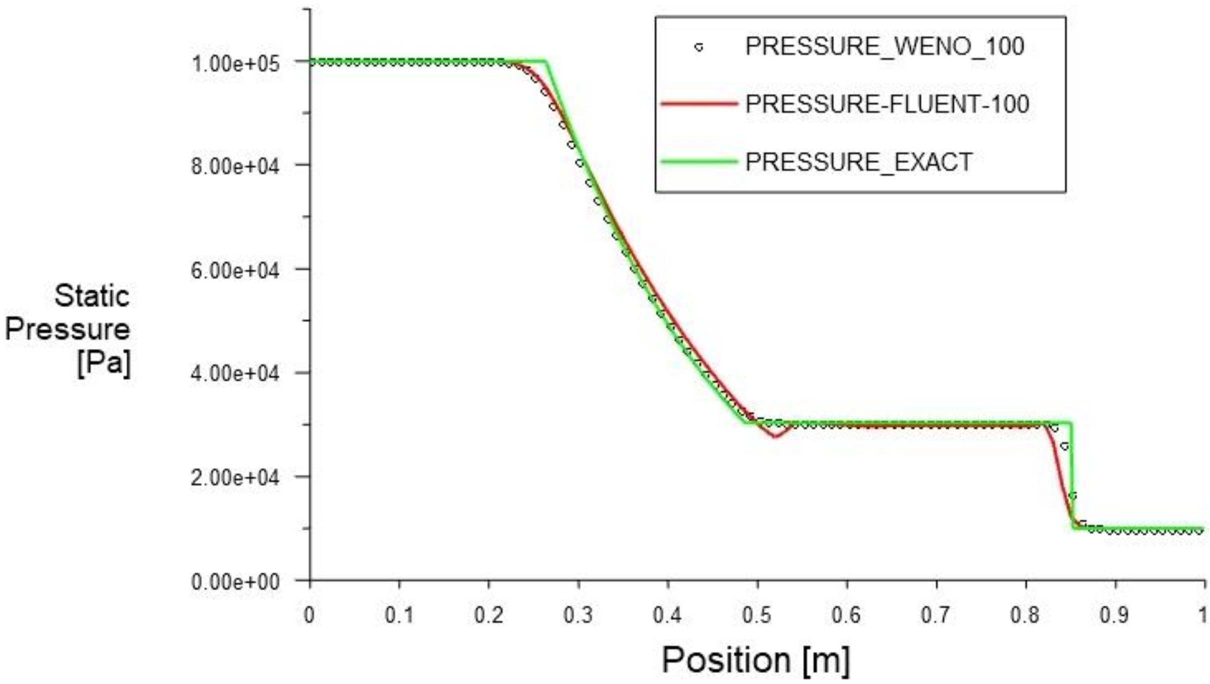

Figure 16. Variation of pressure along the shock tube.

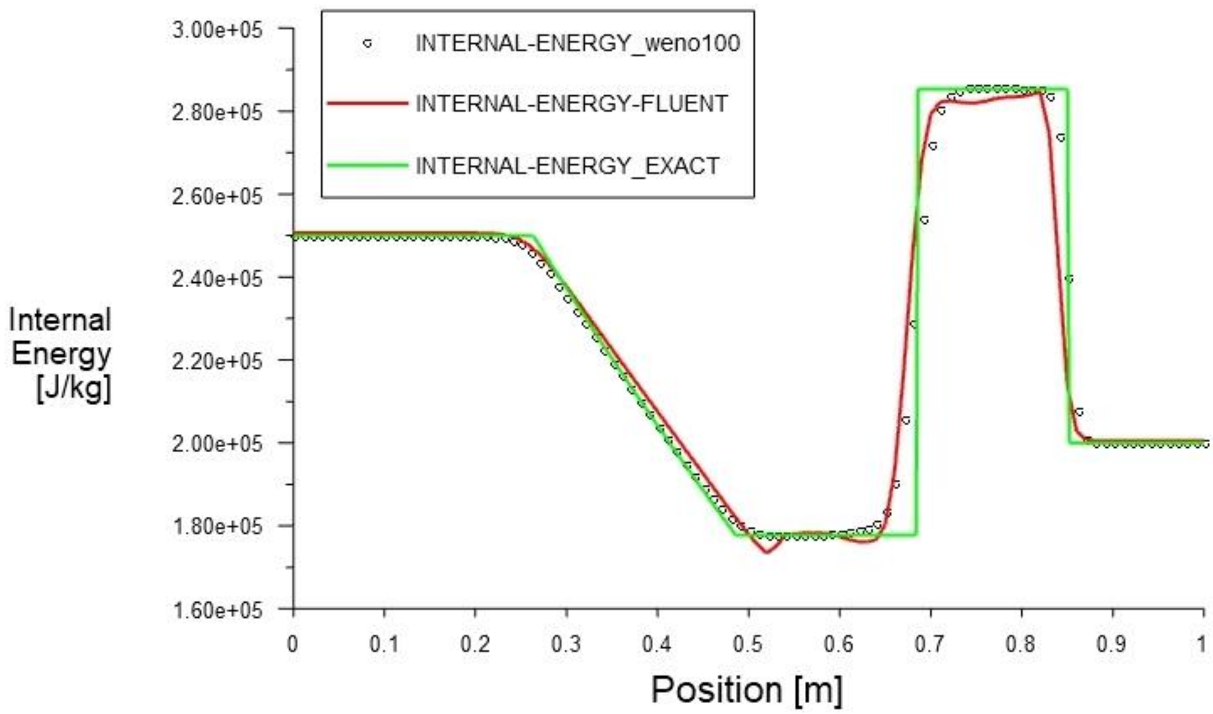

Figure 17. Variation of internal energy along the shock tube.

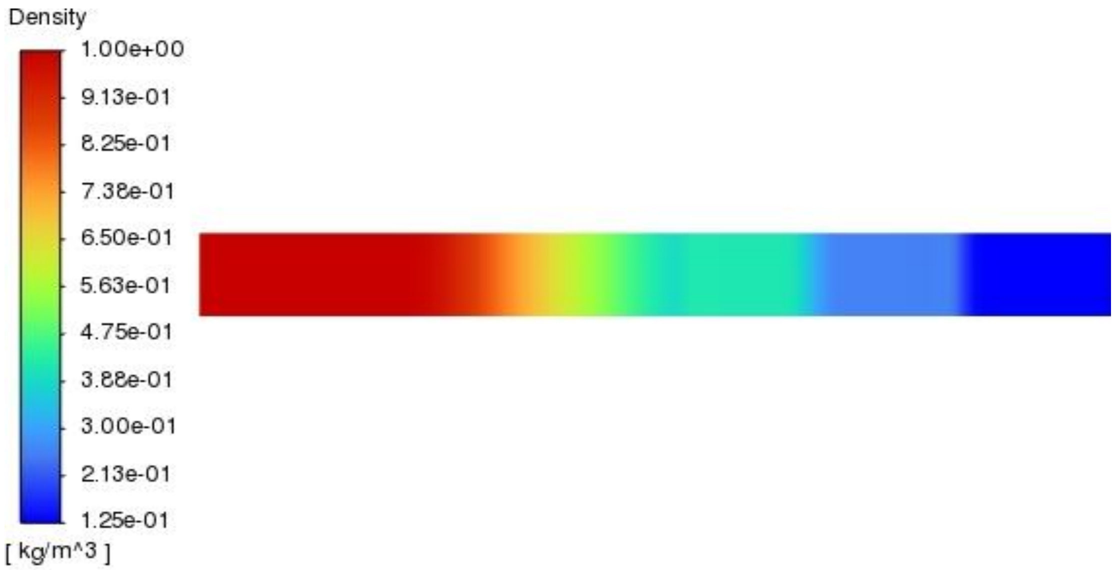

Figure18. Density Contour.

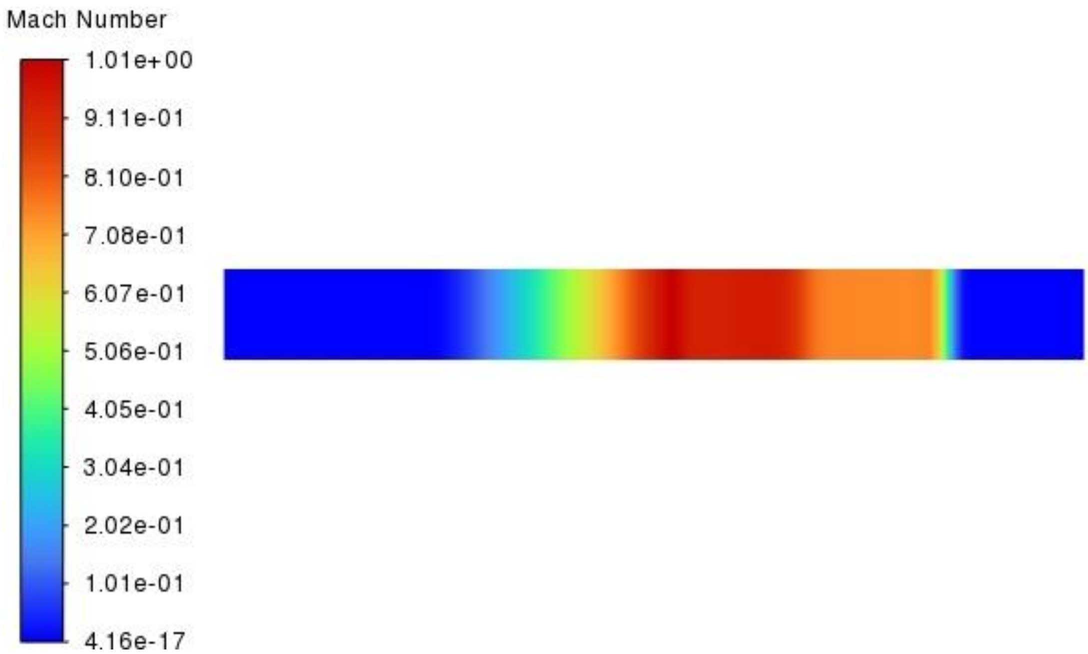

Figure 19. Contour 0f the Mach number.

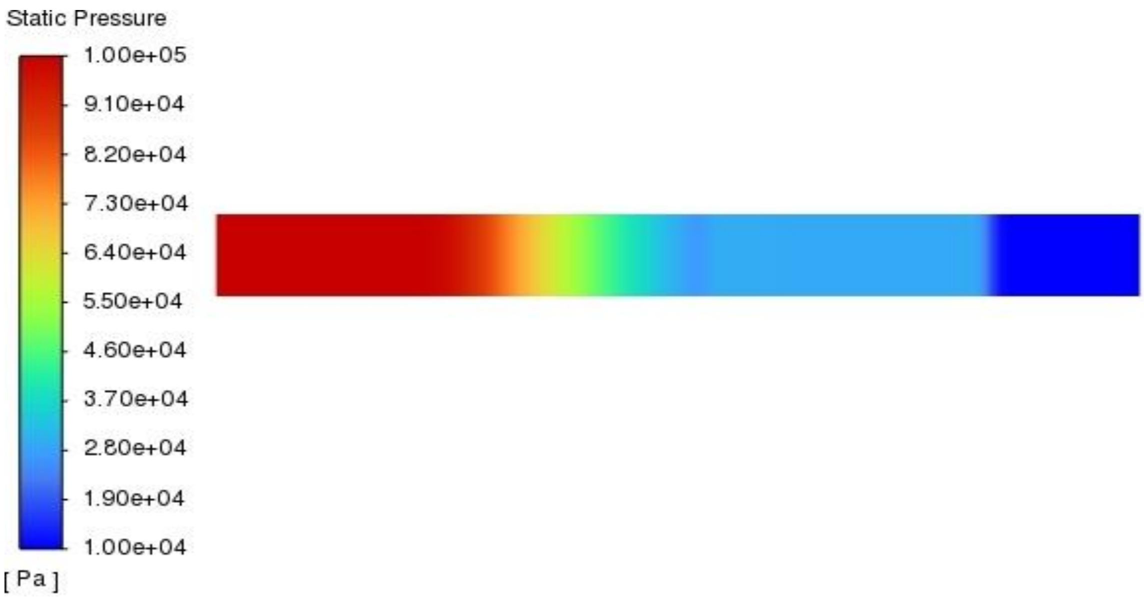

Figure 20. Pressure contour.

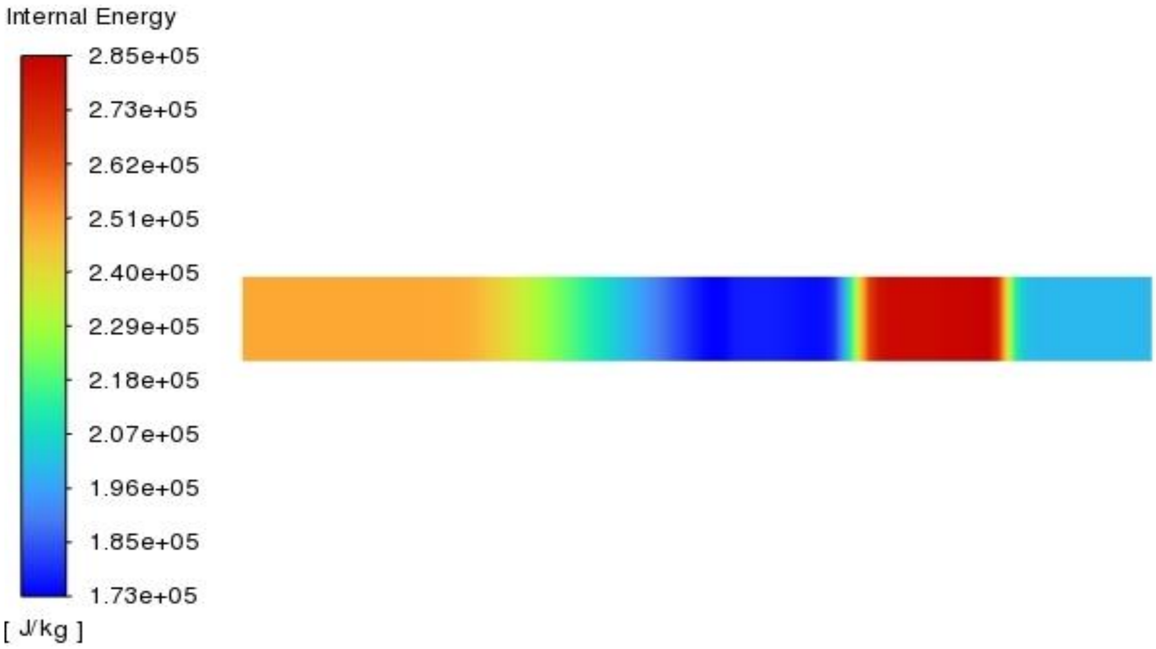

Figure 21. Internal energy contour.

The comparison between the results obtained with Ansys Fluent using a Roe scheme and the results obtained with a 5th order WENO scheme yields the following conclusions.

Figures 14 to 21 depict the evolution of various quantities (density, pressure, Mach number, and energy) as a function of position in the shock tube. These figures allow visualization of how these quantities vary along the tube.

The results obtained with Ansys Fluent using the Roe scheme are not accurate and exhibit oscillations. These oscillations can be attributed to numerical dispersion between the end of region 2 (expansion or rarefaction wave zone) and the beginning of region 3, which is characterized by constant density, pressure, and velocity.

On the other hand, the results obtained with the 5th order WENO scheme are much better, using the same mesh configuration. This indicates that the 5th order WENO scheme produces more accurate and stable results, without the oscillations observed with Ansys Fluent.

It appears that the results from Fluent exhibit more numerical dissipation at the discontinuity contact line, especially at the shock position. Numerical dissipation is an undesirable phenomenon that occurs during the numerical resolution of conservation equations. It can lead to a loss of accurate information about discontinuities, such as the shock line.

The presence of more pronounced numerical dissipations at the shock position may indicate that Fluent with a mesh of 100 nodes does not properly capture the abrupt variations of physical quantities at this location. Numerical dissipations can lead to a loss of information regarding the location and intensity of the shock, resulting in less accurate results.

In contrast, the 5th order WENO scheme shows better results. WENO schemes (Weighted Essentially Non-Oscillatory) are designed to minimize numerical dissipations and more accurately capture discontinuities. This explains the observed improvement with this scheme, including a reduction in numerical dissipations at the discontinuity contact line and a better representation of the shock.

It seems that we want to express that the difference in results between Fluent using a second-order Upwind discretization scheme and WENO 5 is not attributed to the Roe scheme. Instead, we believe that the weakness lies in the Upwind scheme itself, especially with a mesh size of 100 nodes, as it may not accurately capture all variations.

To further analyze and support our claim, we can consider the following points:

Compare Roe chart with WENO: Highlight the fact that the Roe scheme yields good results when combined with the WENO scheme. This indicates that the Roe scheme itself is not the main source of discrepancy.

Limitations of the Upwind scheme: Discuss the inherent limitations of the second-order Upwind scheme. For instance, the Upwind scheme is known to introduce numerical diffusion, which can result in a loss of accuracy when capturing sharp variations or gradients.

Mesh size and resolution: Make sure that with a mesh size of 100 nodes, the resolution may not be sufficient to accurately represent the features and variations of the flow.

Mesh results 1-200

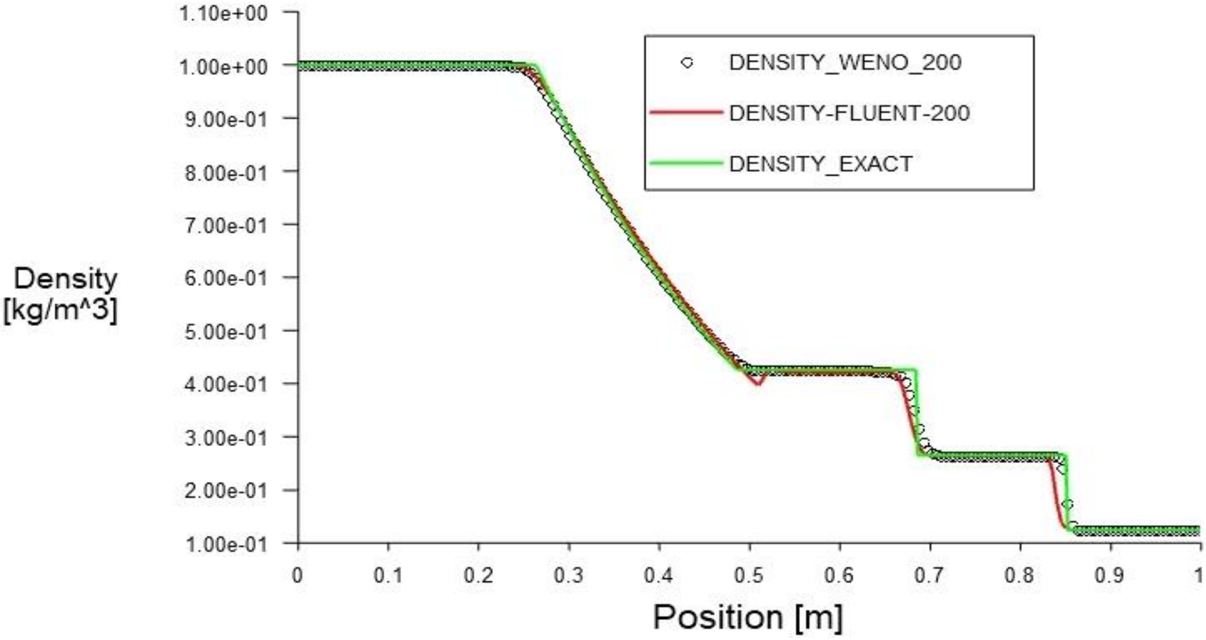

Figure 22. Variation of density along the shock tube.

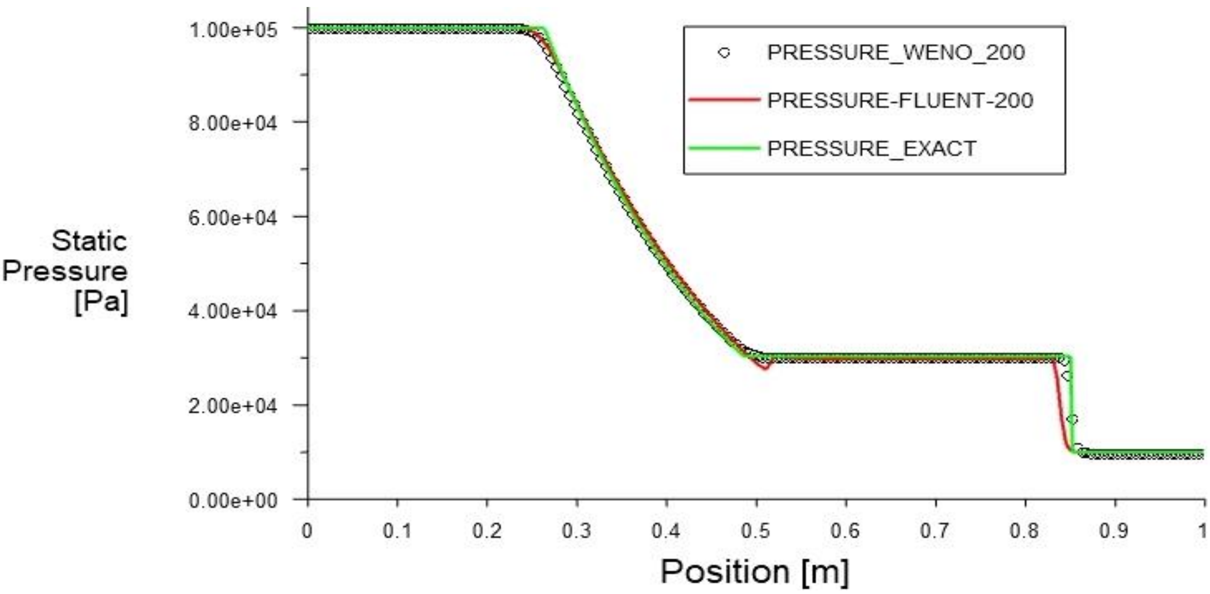

Figure 23. Variation of pressure along the shock tube.

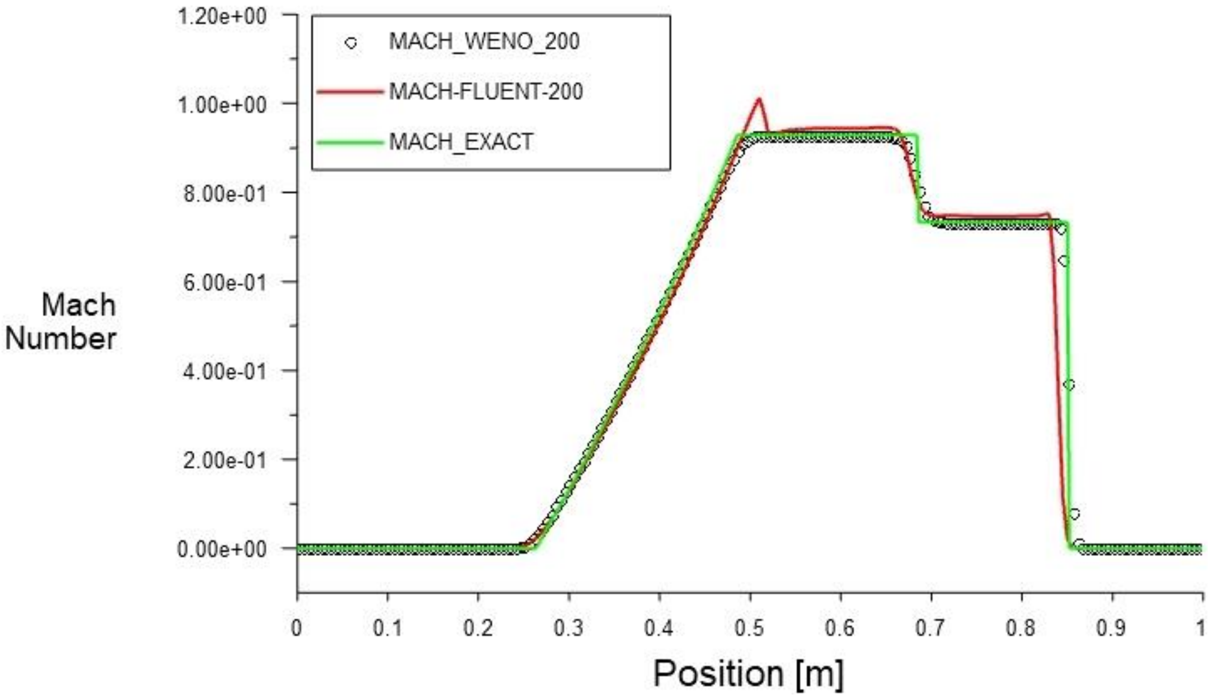

Figure 24. Variation of the Mach number along the shock tube.

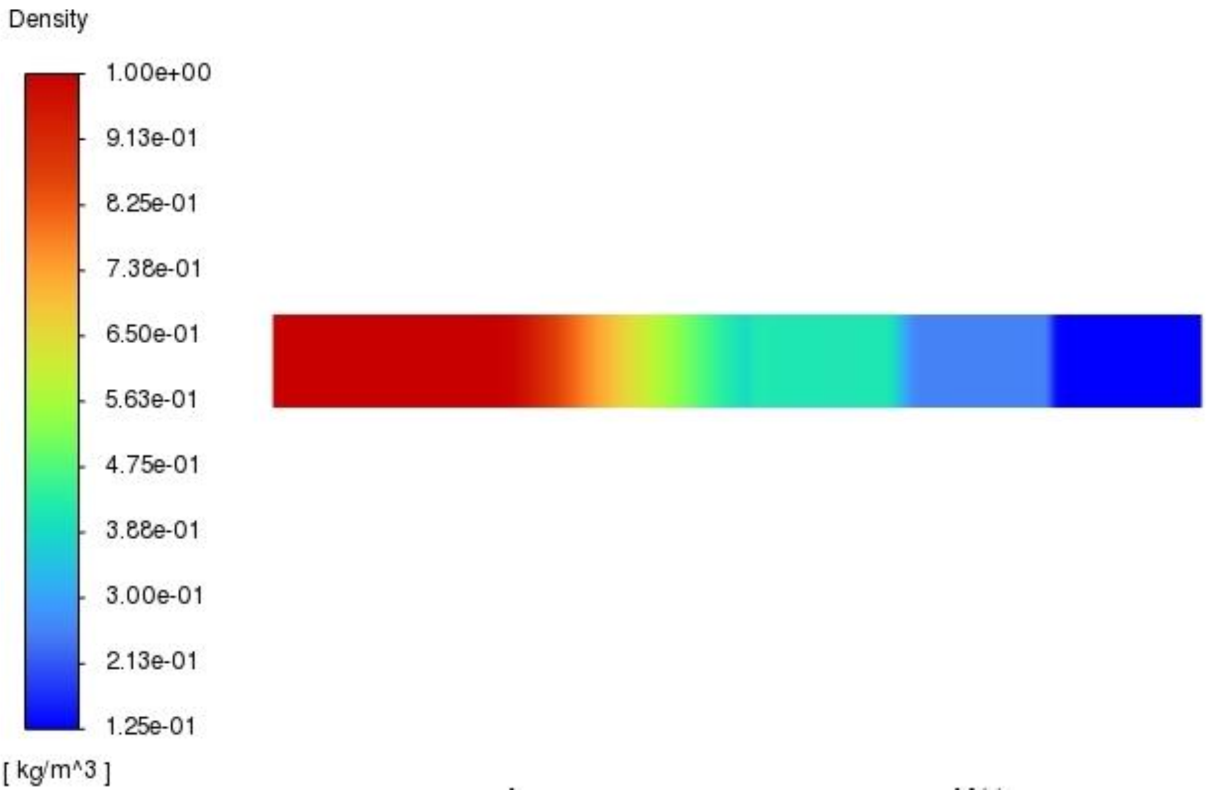

Figure 25. Density contour.

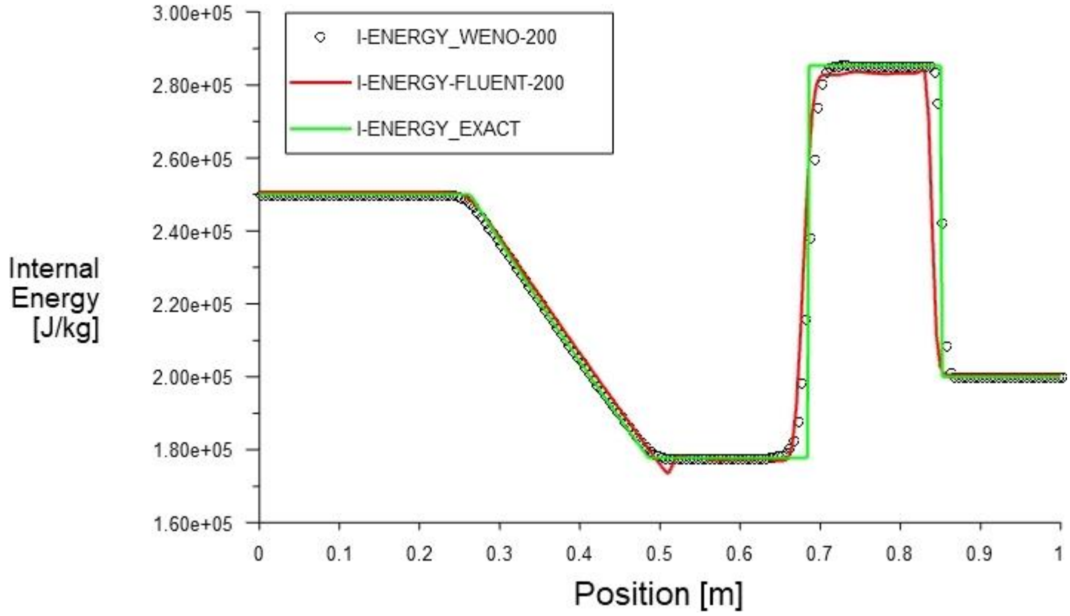

Figure 26. Variation of the internal energy along the shock tube.

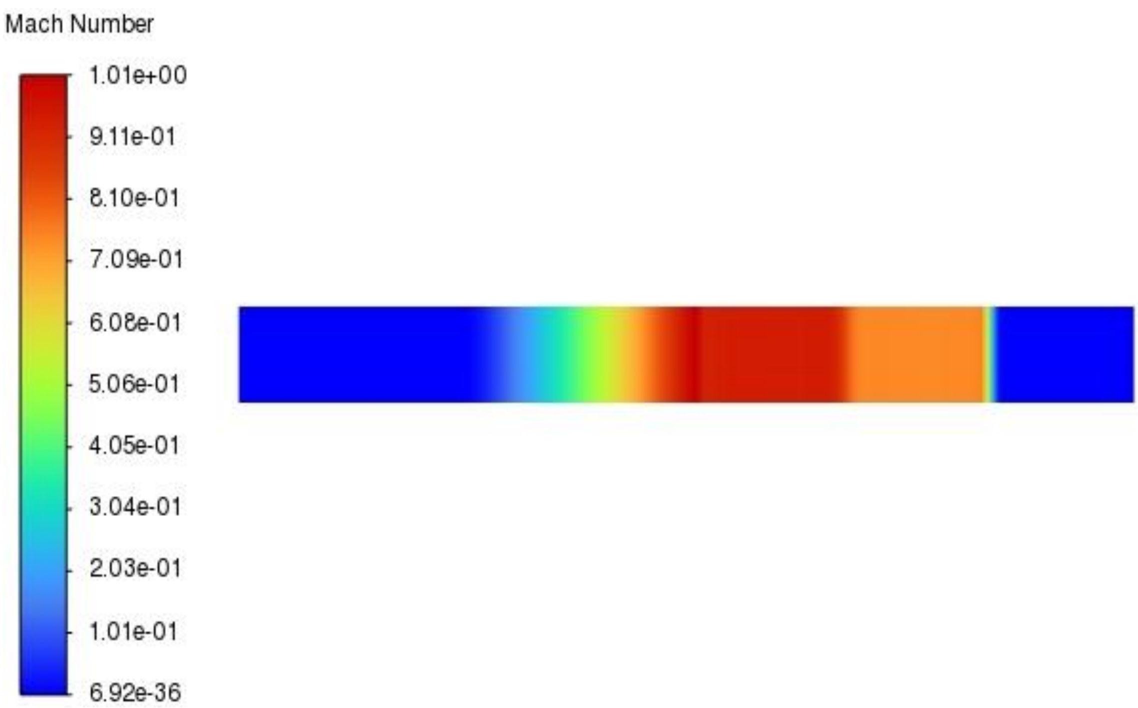

Figure 27. Mach number contour.

Figure 28. Pressure contour.

Figure 29. Internal energy contour.

The results obtained using the second-order Upwind discretization scheme in the Fluent code, with meshes of 200 nodes (figures 22-29), showed numerical dispersion between the end of zone 2 and the beginning of zone 3 of the shock tube. This numerical dispersion is manifested by an entropy variation between these two regions, where entropy increases in zone 2 and remains constant in zone 3. Although the finer mesh of 200 nodes allowed for a slight improvement in Fluent results, the numerical oscillation was not significantly improved. This suggests that the Roe scheme used in Fluent may require more significant entropy correction to better capture the complex flow variations in the shock tube.

The numerical dissipation observed in the Fluent code results using the Roe scheme may be related to the issue of inadequate capture of discontinuities, such as shock and contact lines. This phenomenon is often attributed to a lack of appropriate entropy correction in the numerical scheme. The Roe scheme, although widely used in fluid mechanics, is known to present difficulties in handling discontinuities. Indeed, the Roe scheme can produce non-physical solutions in certain regions of the flow, especially when the flow transitions from supersonic to subsonic, as is the case in the shock tube.

The problem lies in the fact that the Roe scheme does not always ensure entropy growth across discontinuities. This violation of the entropy principle results in the appearance of numerical oscillations and excessive dissipation, as observed in the Fluent code results for the shock tube. To address this problem, specific entropy corrections have been developed for the Roe scheme. These corrections aim to ensure that entropy grows monotonically across discontinuities, thereby eliminating non-physical solutions.

Among the main entropy correction methods for the Roe scheme, the following can be cited:

Harten's entropy limiter: This method introduces an entropy limiter that prevents the creation of new local maxima and minima in the solution, thus ensuring monotonic entropy growth.

Roe-Sweby scheme: This approach directly modifies the Roe numerical fluxes to ensure entropy growth while retaining the conservation and high-resolution properties of the original scheme.

The roe scheme with correction by diffusion: This method adds an additional numerical diffusion term, proportional to the entropy jump, to stabilize the solution and ensure entropy growth. Implementing one of these entropy corrections in the Fluent code could potentially improve the capture of discontinuities and reduce the numerical dissipation observed in the shock tube simulation results.

This would lead to more accurate results in better agreement with the exact solution. Although entropy corrections add extra complexity to the numerical scheme, they are often necessary to properly handle compressible flows with pronounced discontinuities, as in the case of the studied shock tube.

However, significant improvement has been observed using the 5th-order WENO scheme. With the same number of nodes, the WENO scheme produced nearly exact results and better reproduced the exact solution.

It accurately captured variations in density, pressure, velocity, and energy along the shock tube, except for some slight differences in the evolution of internal energy. The WENO scheme proved to be a more accurate and better-suited method for this simulation, with superior ability to capture flow details, even with a coarser mesh.

Mesh results 1-1000

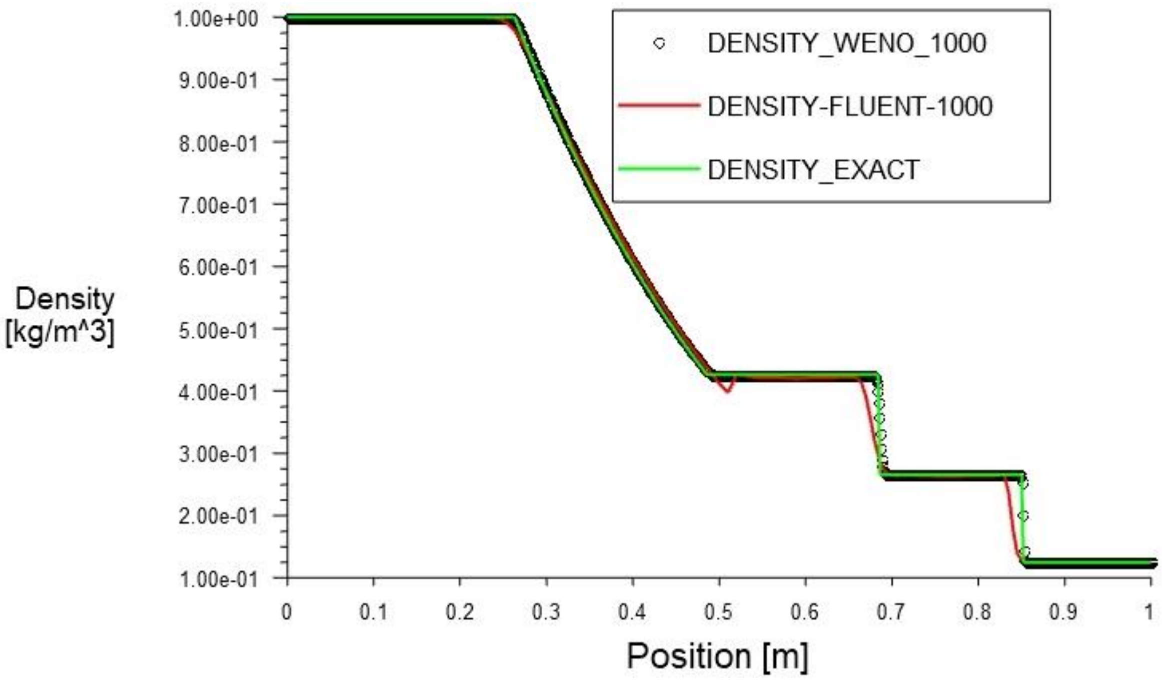

Figure 30. Variation of density along the shock tube.

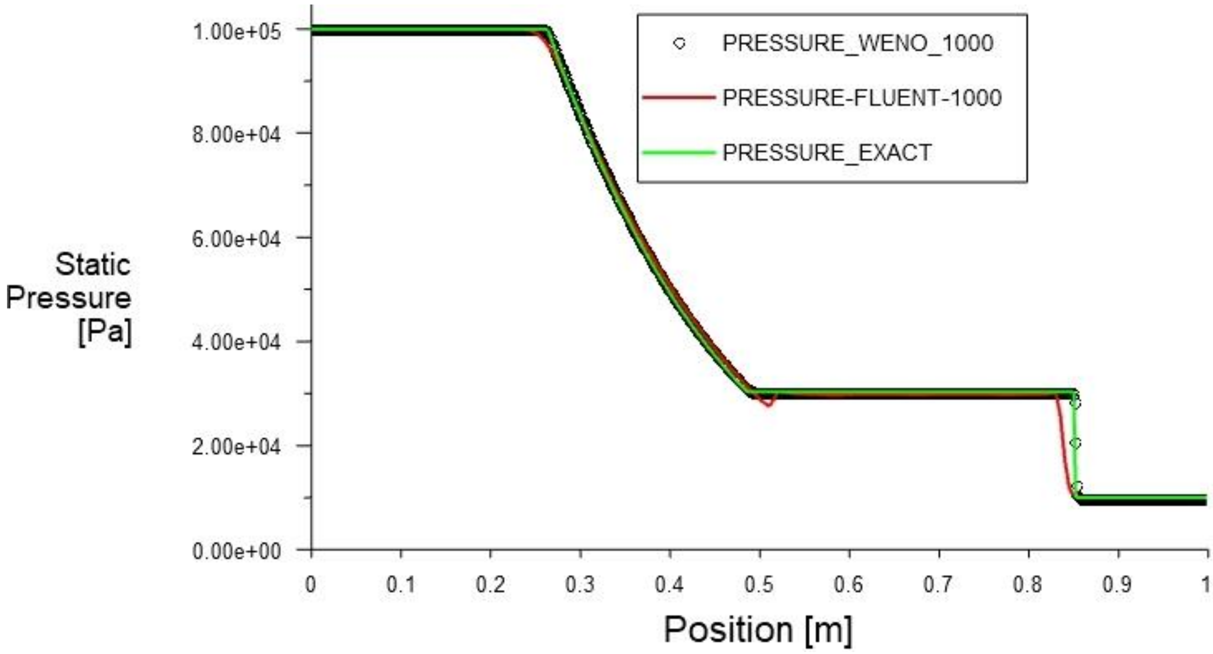

Figure 31. Variation of pressure along the shock tube.

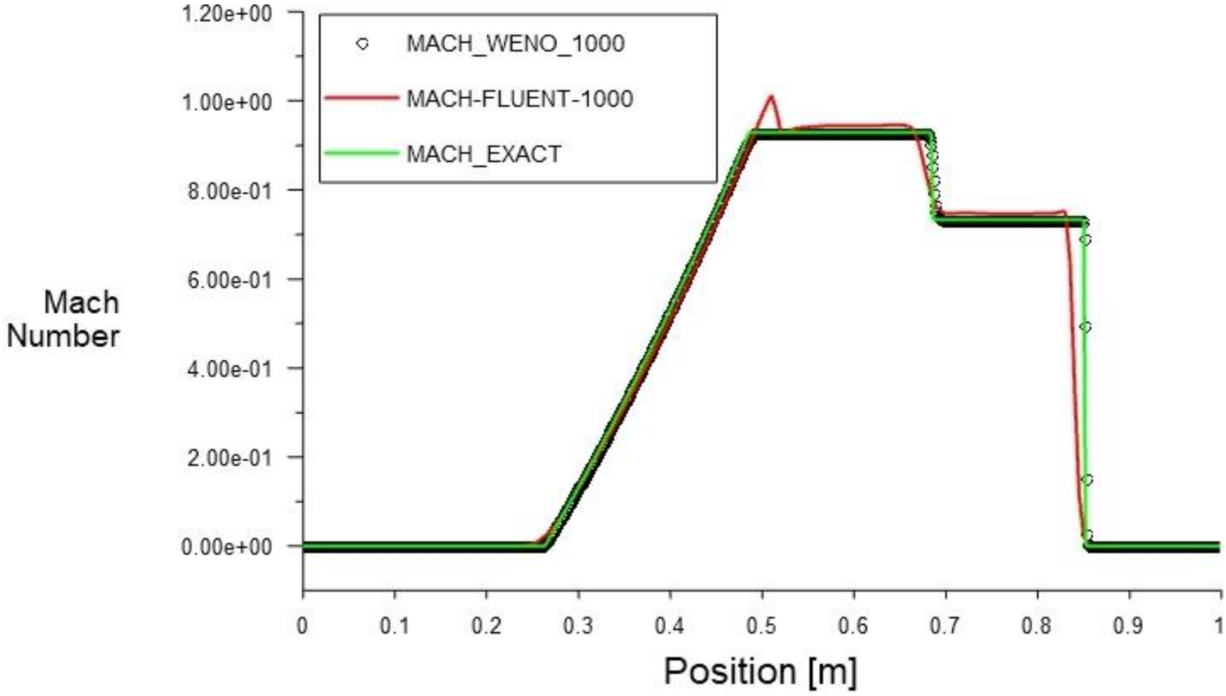

Figure 32. Variation of the Mach number along the shock tube.

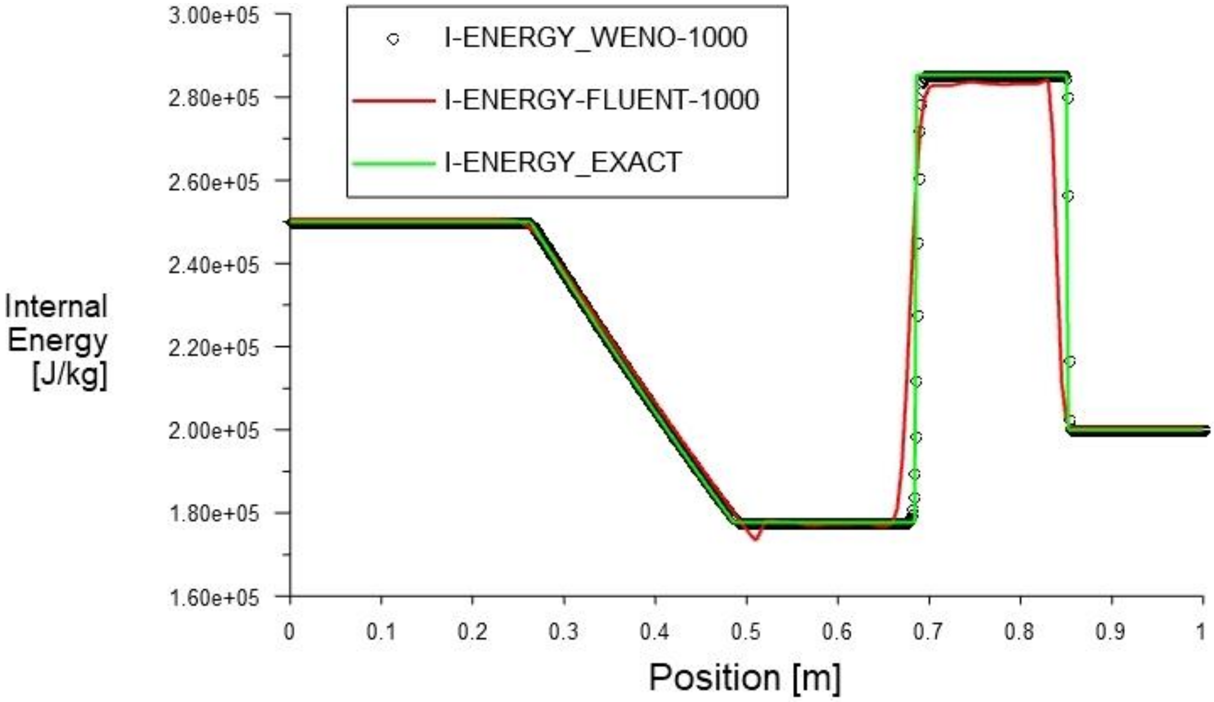

Figure 33. Variation of the internal energy along the shock tube.

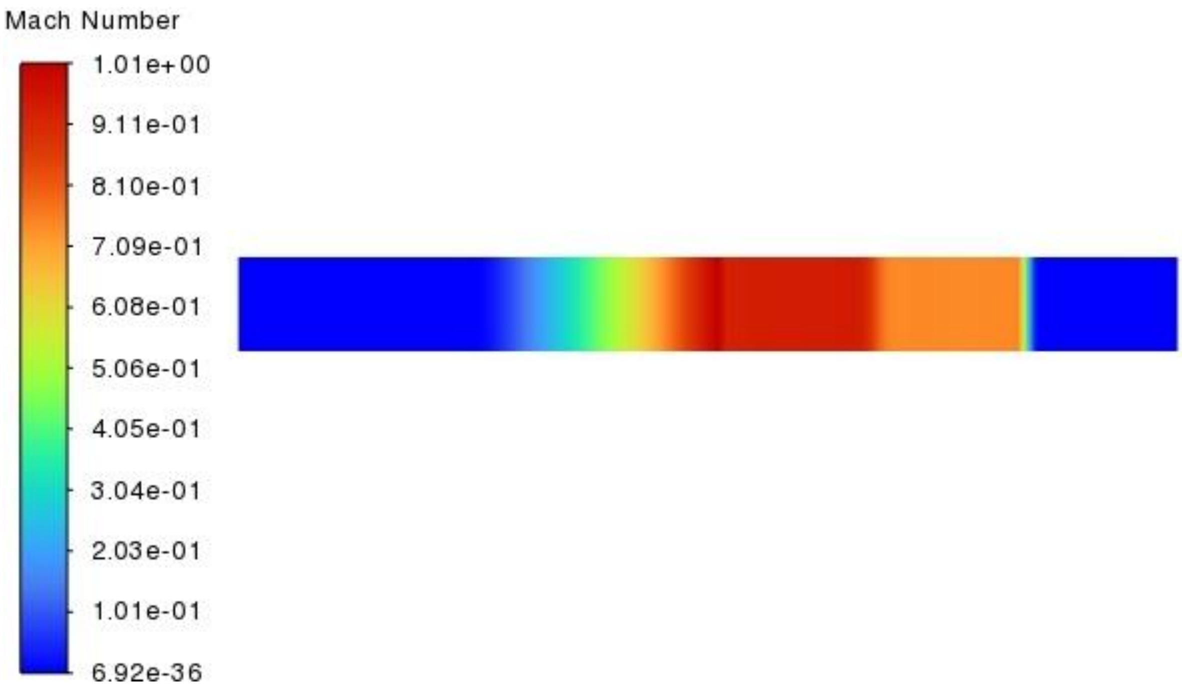

Figure 34. Mach number contour.

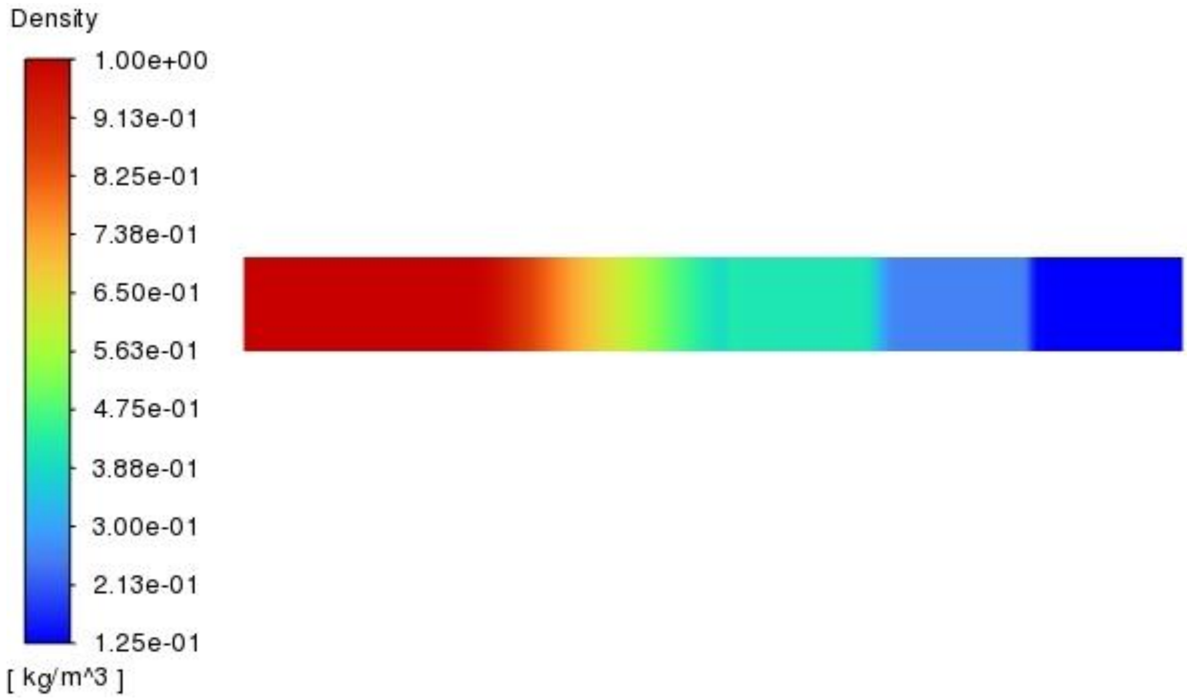

Figure 35. Density contour.

Figure 36. Pressure contour.

Figure 37. Internal energy contour.

A comparison between Ansys Fluent and the WENO 5 scheme for studying numerical dispersion and diffusion in a shock flow problem is presented in figures 30-37. Despite increasing the number of nodes to 1000, Ansys Fluent shows some improvement in predicting numerical dispersion and diffusion, but this improvement is not sufficient.

We also observe that dispersion persists even with this mesh refinement, which is unexpected. Additionally, we observe that the WENO 5 scheme approaches the exact solution excellently and effectively detects all phenomena present in the shock flow demonstrating its power.

It is interesting to note that the WENO 5 scheme does not seem to require a refined mesh to produce good results, unlike Ansys Fluent. This may suggest that the WENO 5 scheme is more suitable for capturing shock flow phenomena without being too affected by mesh resolution.

These observations demonstrate that the WENO 5 scheme offers significant advantages over Ansys Fluent in simulating shock flows, particularly in terms of accuracy and robustness regarding mesh resolution.

These results are important for guiding the choice of the most appropriate numerical method for this type of problem.

Mesh results 1-5000

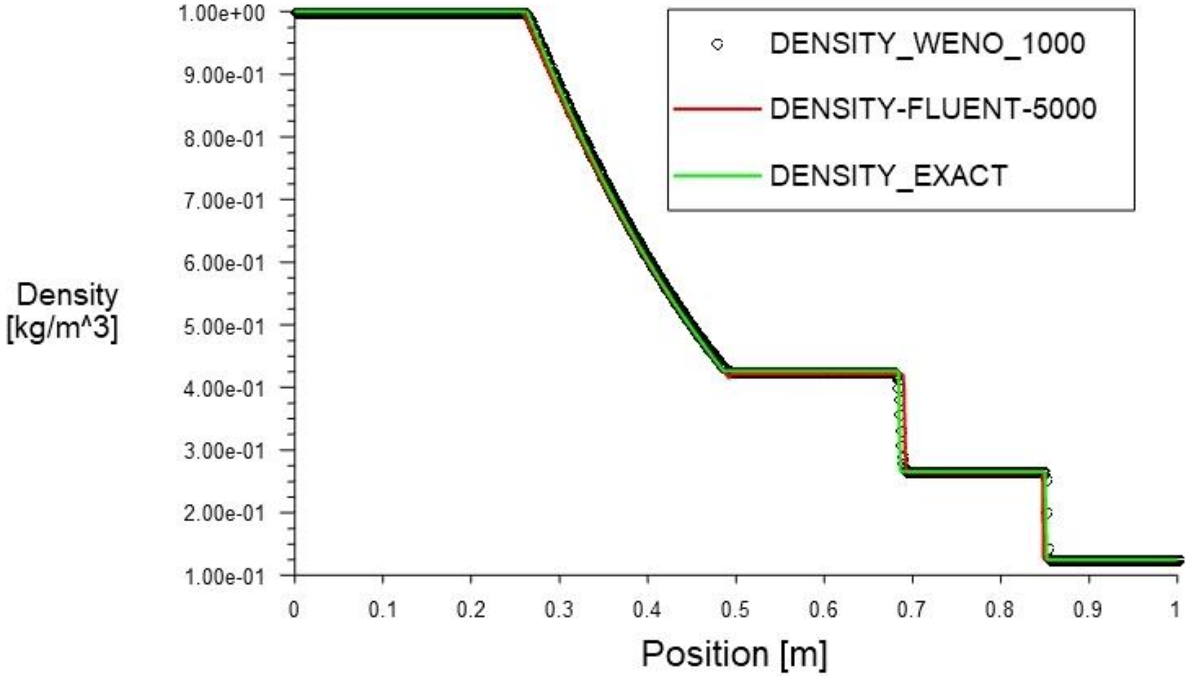

Figure 38. Variation of density along the shock tube.

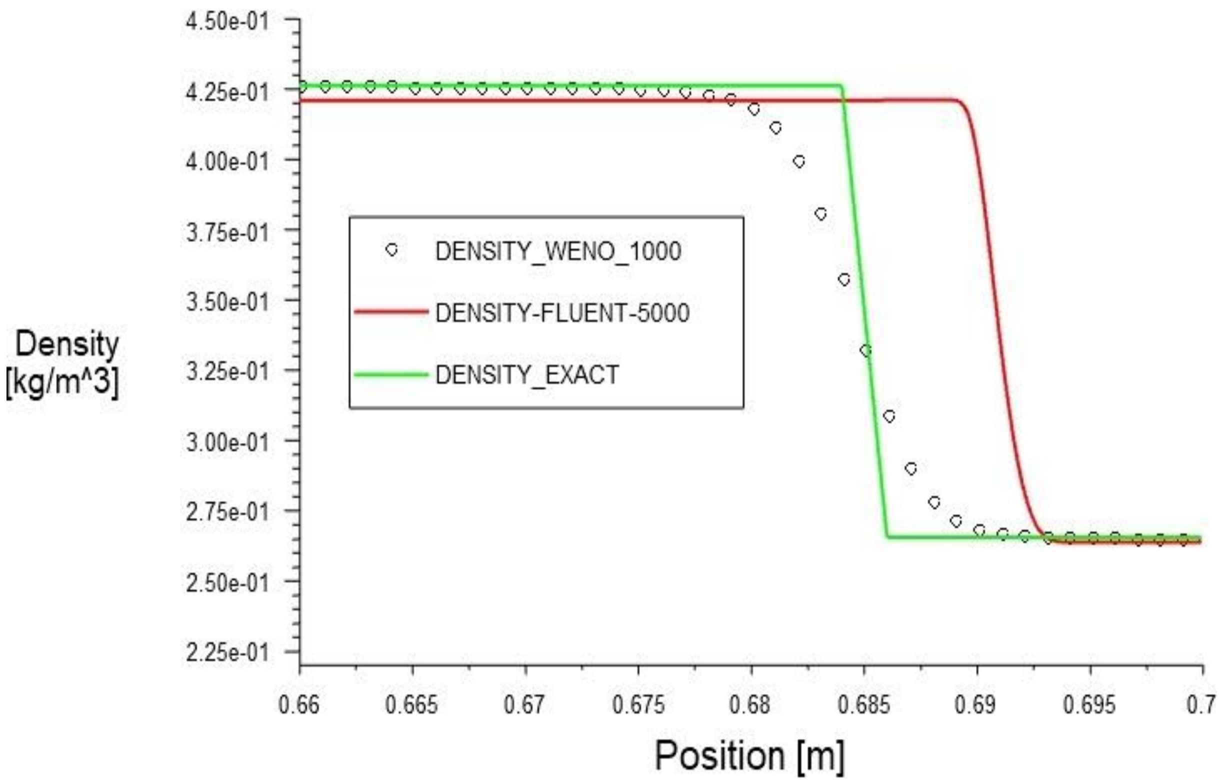

Figure 39. Zoom view of density .

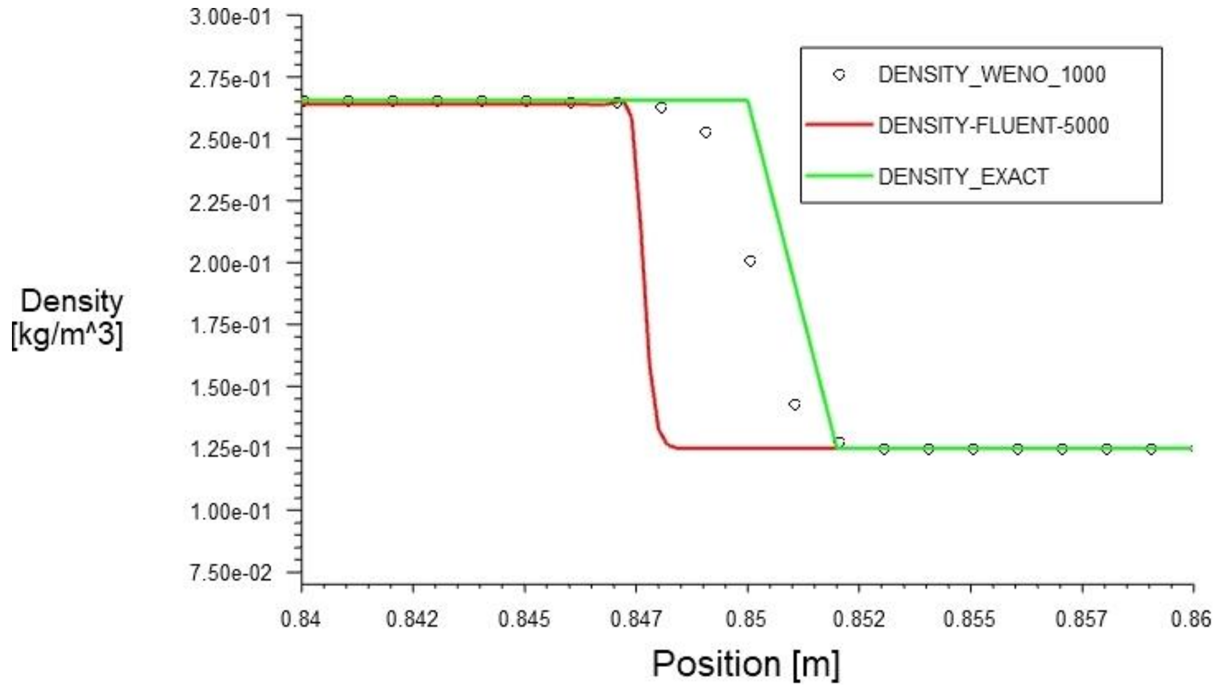

Figure 40. Zoom view of density.

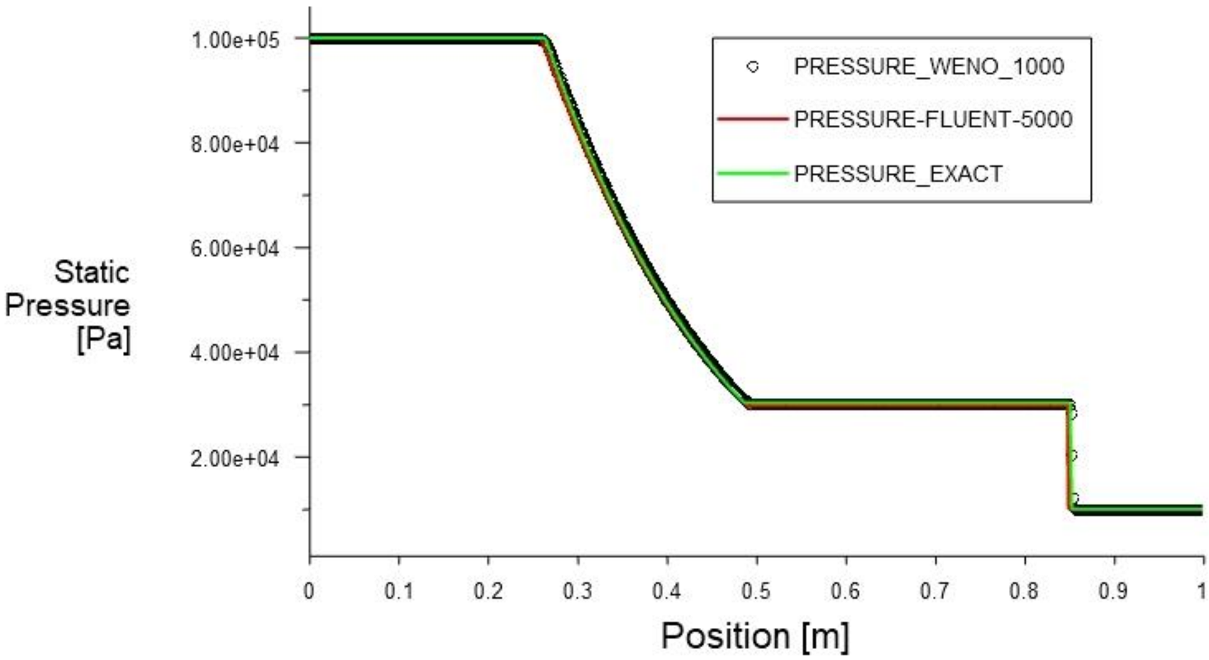

Figure 41. Variation of pressure along the shock tube.

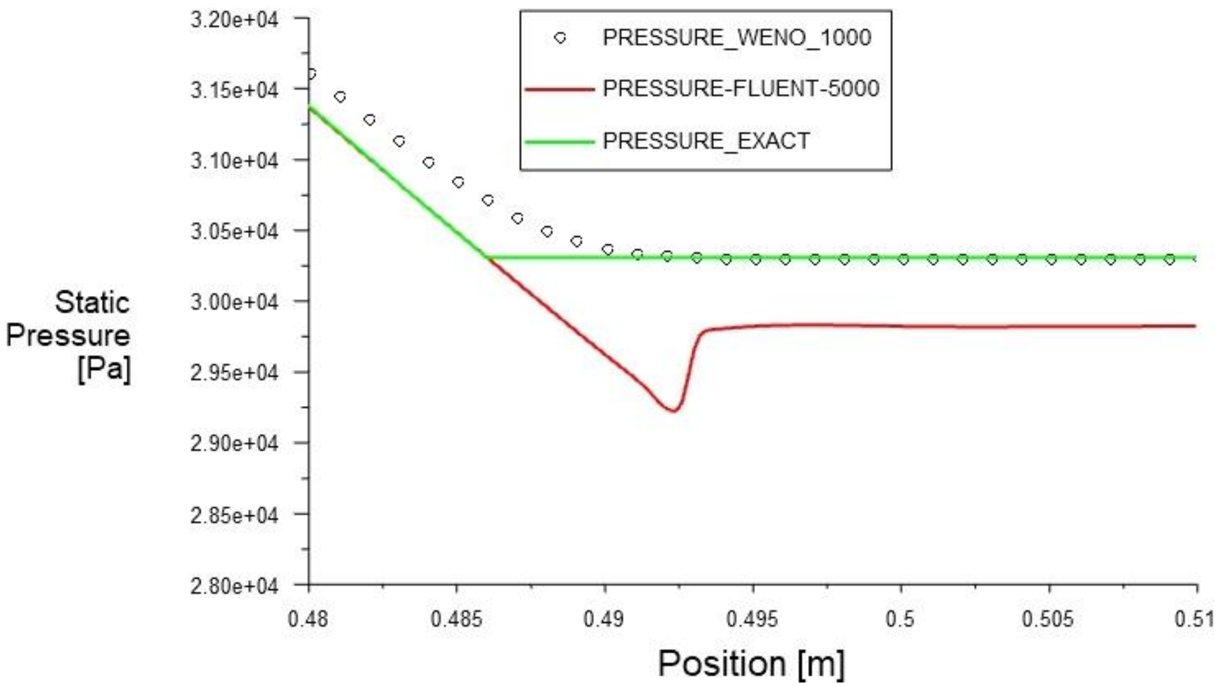

Figure 42. Zoom view of pressure.

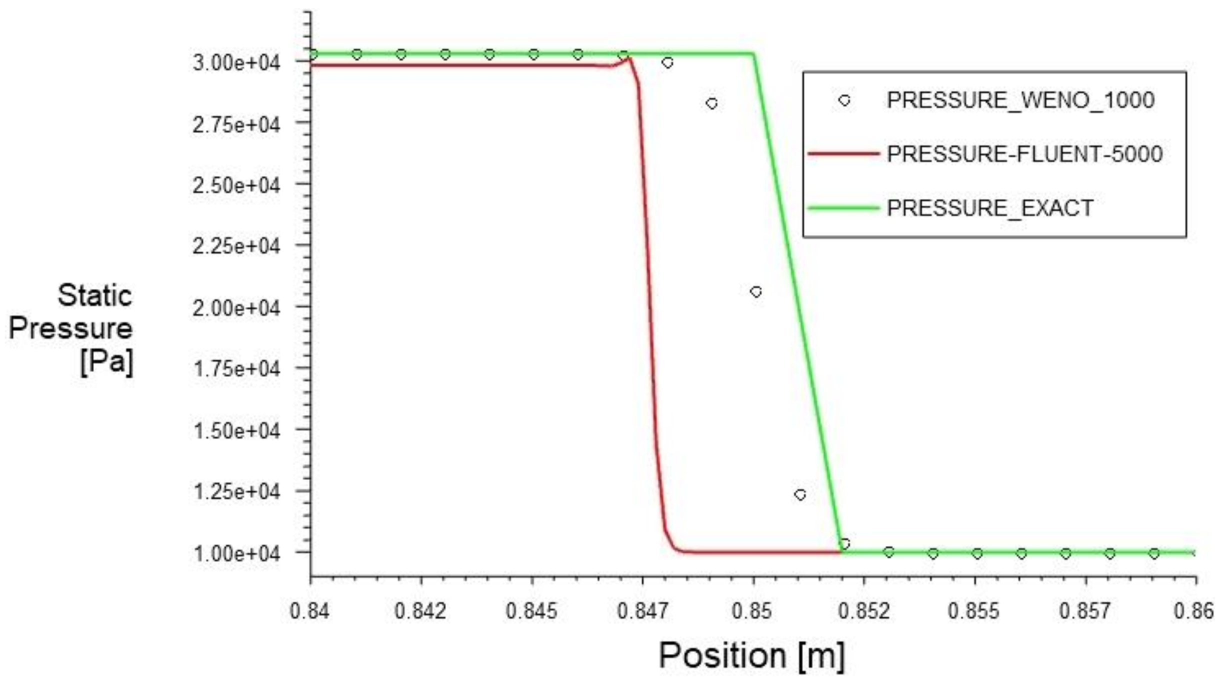

Figure 43. Zoom view of pressure.

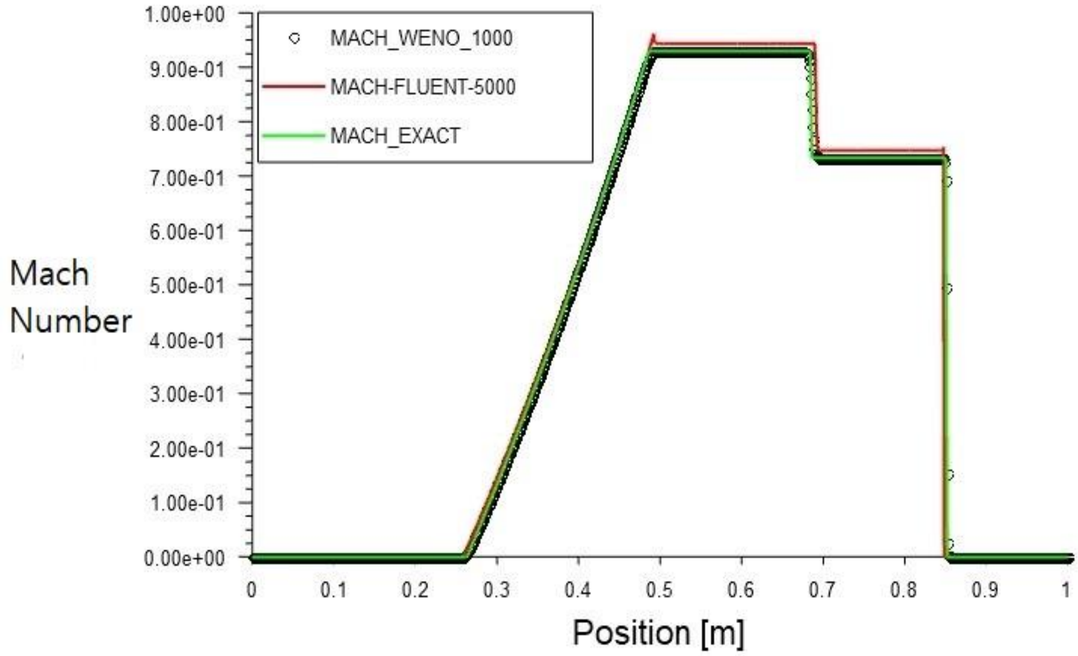

Figure 44. Variation of the Mach number along the shock tube.

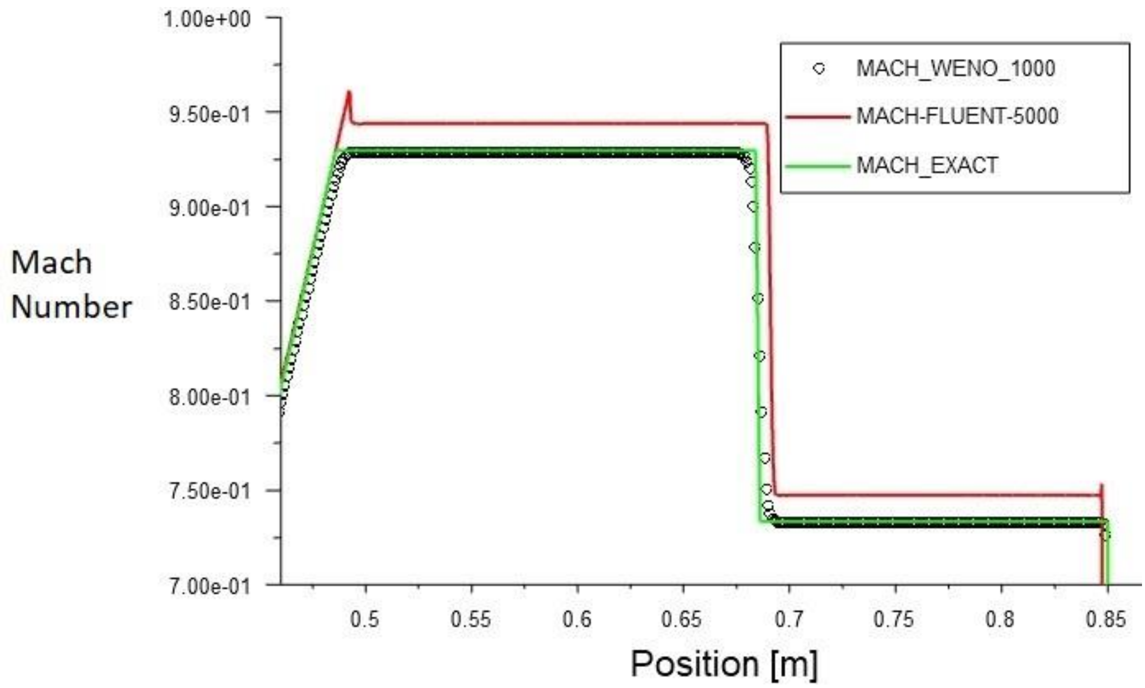

Figure 45. Zoom view of mach number

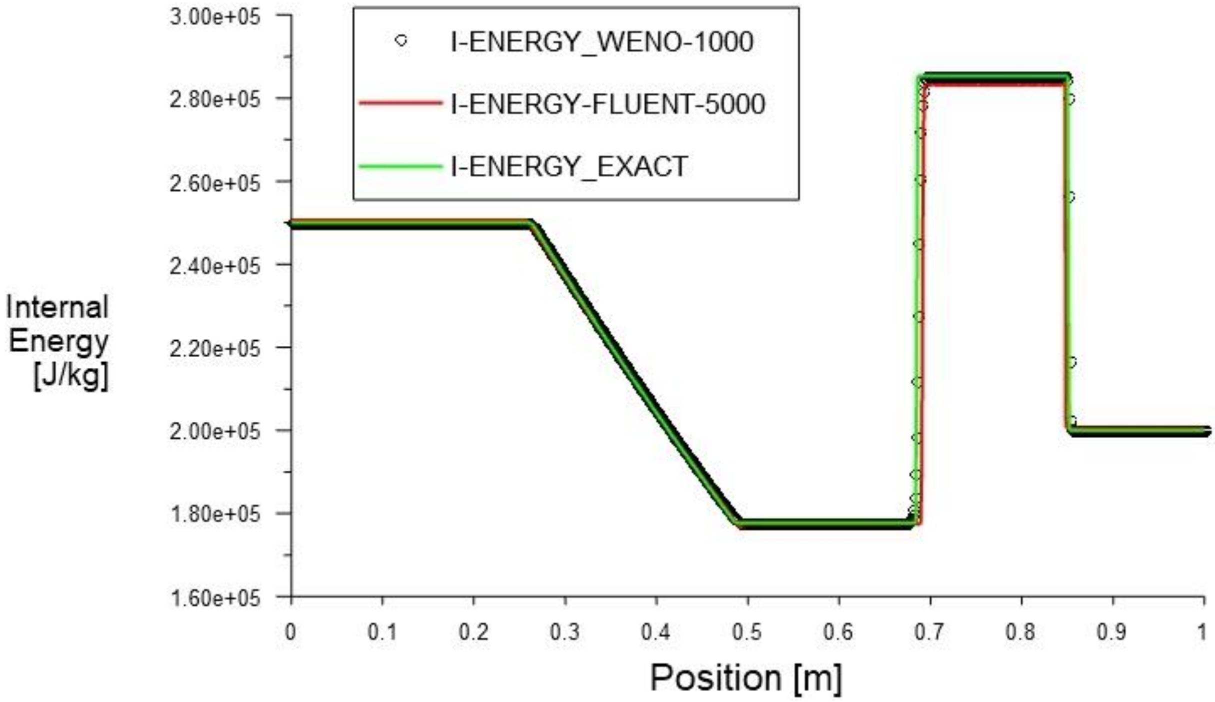

Figure 46. Variation of the internal energy along the shock tube.

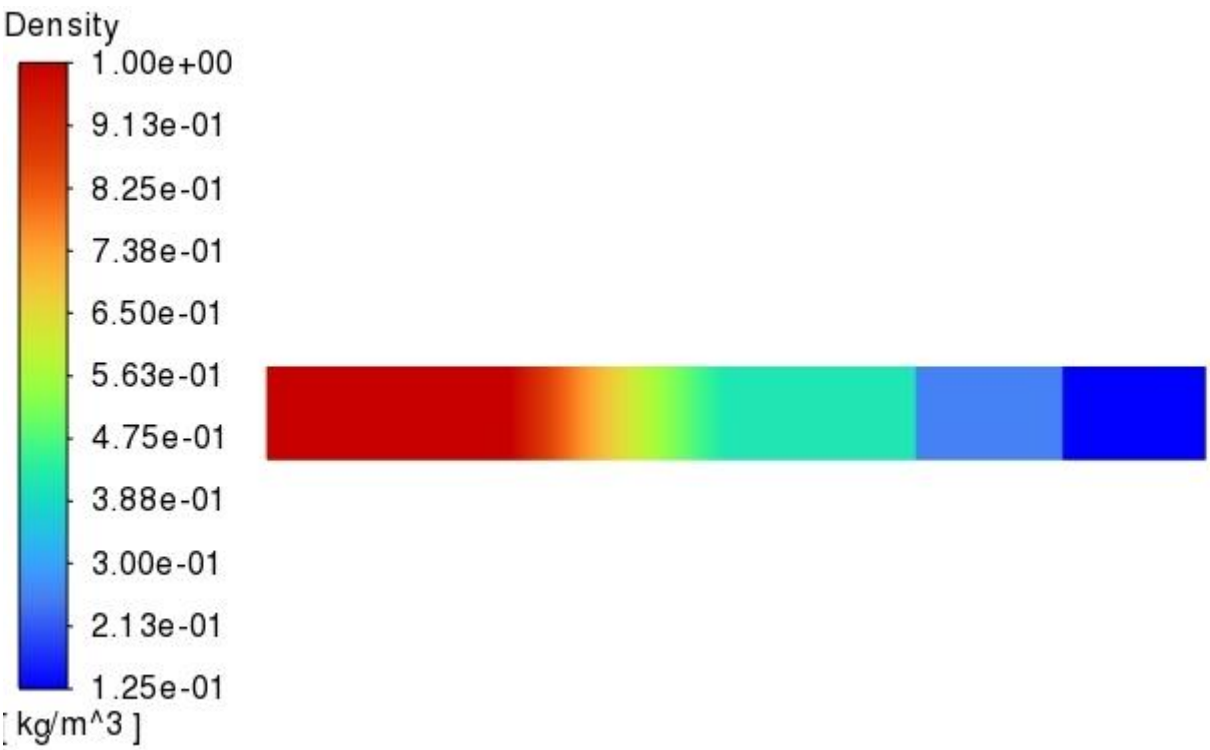

Figure 47. Density contour.

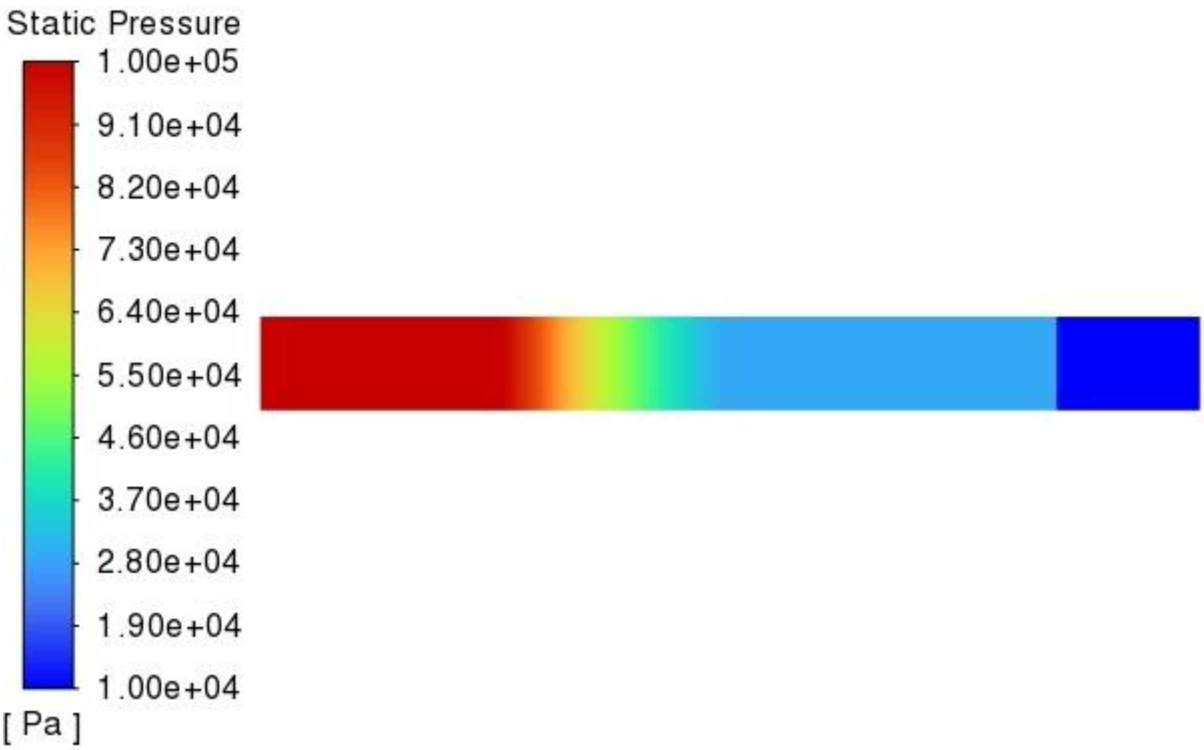

Figure 48. Pressure contour.

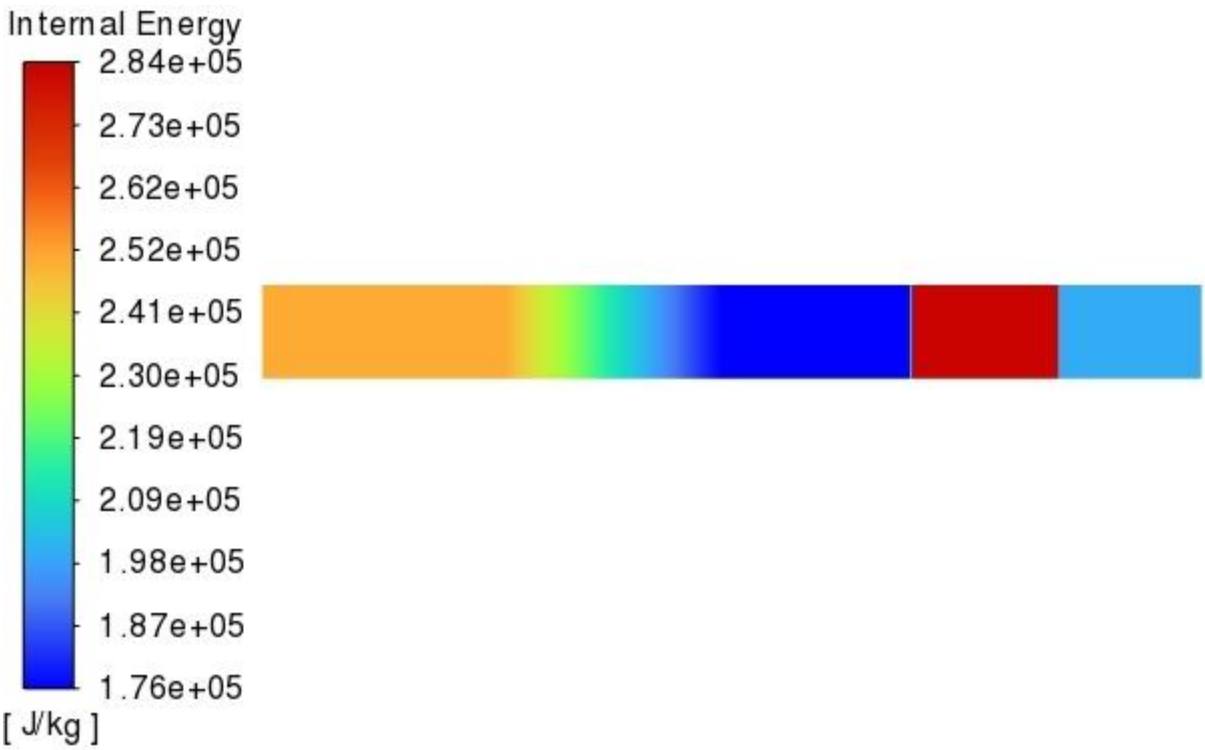

Figure 49. energy contour.

Figure 50. mach number contour.

It appears that when you increased the mesh in Ansys Fluent to 5000 nodes while keeping the WENO5 scheme mesh at 1000 nodes, the results significantly improved. Indeed, Figures 38 to 50 show that numerical dispersion became very low and numerical diffusion minimal with the finer mesh of Ansys Fluent.

However, you point out that even with this highly refined mesh of 5000 nodes, the performance of Ansys Fluent remains inferior to that of the WENO5 scheme, which, when used with only 1000 nodes, produces excellent results.

You note that in the standard study of the one-dimensional Riemann problem (Sod shock), researchers typically use a maximum of only 200 nodes. Therefore, in this simple case, it cannot be considered that Ansys Fluent is truly capable of producing good results with a much finer mesh of 5000 nodes. These observations strengthen the advantage of the WENO5 scheme over Ansys Fluent for simulating shocked flows.

The WENO 5 scheme appears to accurately capture flow phenomena, even with a much coarser mesh than what is required for Ansys Fluent. This demonstrates the power and robustness of the WENO 5 scheme in this type of problem.

General conclusion

General conclusion

This study focuses on comparing two widely used numerical codes in fluid dynamics: Ansys Fluent, which uses a second-order Upwind scheme with Roe flux decomposition, and an in-house code employing a fifth-order WENO scheme with Roe flux decomposition, within the framework of calculating flow in a Sod shock tube configuration. Both schemes are implemented in the finite volume method, enabling the resolution of complex geometries.

The comparison between these two codes was conducted by concentrating on three essential aspects: result accuracy, mesh consumption, and computation time. The study focuses on supersonic flows with shock waves, where the second-order Upwind scheme with Roe flux decomposition in Fluent is renowned for its robustness. The choice of the optimal scheme will depend on the specificities of the problem to solve and the researcher's priorities (accuracy, mesh consumption, computation time). It's important to note that configuring each scheme's parameters can influence the results. The study should explore how these parameters impact the performance of both schemes.

Regarding result accuracy, it appears that the WENO 5 scheme consistently offers excellent precision, particularly in challenging areas like contact discontinuities and pure shock positions. However, when using Fluent with mesh sizes of 100 or 200 nodes, the results are unsatisfactory and significantly deviate from exact solutions, even compared to the WENO scheme. This is mainly due to the presence of numerical dispersion in the form of Gibbs oscillations and significant numerical diffusion at different positions of discontinuity or shock.

Nevertheless, there is some improvement when using a mesh of 1000 nodes, with less numerical diffusion dispersion. Results significantly improve for Fluent with a larger mesh of 5000 nodes. Based on this observation, one can conclude that the WENO 5 scheme outperforms Fluent in terms of accuracy, especially when comparing results obtained with the same number of mesh nodes. Fluent seems to require a finer mesh to achieve comparable accuracy, and even in such cases, it may still encounter issues with dispersion and numerical diffusion.

It's crucial to note that the conclusions drawn from this comparison are specific to the Sod shock tube configuration and the considerations made in terms of accuracy. Other factors, such as computational efficiency and mesh consumption, must also be taken into account when choosing the most suitable scheme for a particular flow problem

Indeed, it's noteworthy that results obtained with a mesh of 5000 nodes in Fluent, although somewhat satisfactory, are less accurate than those obtained with a mesh of 400 nodes using the WENO scheme. This indicates that the mesh node requirement in Fluent to achieve results comparable to those of the WENO scheme is approximately 13 to 20 times higher.

Such an increase in mesh consumption is generally impractical and leads to a significant increase in computation time.

This further underscores the advantage of the WENO scheme in terms of computational efficiency. By using a lower mesh count, it's possible to obtain accurate results, thereby reducing both simulation complexity and the required computation time.

Therefore, it's essential to consider these practical aspects, such as mesh consumption and computation time, when selecting a numerical scheme for a specific application. The WENO scheme offers both high accuracy and relatively good computational efficiency, making it an attractive choice in many cases.

Regarding computation time, it's noteworthy that for Fluent, the computation times for mesh sizes of 100, 200, 1000, and 5000 nodes respectively are approximately 2.15 s, 4 s, 19.91 s, and 140 seconds. For the WENO scheme, for mesh sizes of 100, 200, 500, and 1000 nodes respectively, the computation times are 0.11 s, 0.38 s, 2.30 s, and 9.04 seconds. Considering acceptable results for both codes, it can be observed that the computation time for Fluent is approximately 16 to 60 times longer than that of the WENO scheme, depending on the level of result accuracy acceptance.

This further reinforces the advantage of the WENO scheme in terms of computational efficiency. Not only does it provide accurate results with a lower mesh count, but it also significantly reduces the computation time required to obtain these results.

Therefore, it's crucial to consider both result accuracy and computation time when choosing a numerical scheme for a given application. The WENO scheme offers an interesting compromise between accuracy and computational efficiency, making it an attractive option for many simulations.

References

References

[1] T. Horvath, "Experimental aerothermodynamics in support of the columbia accident investigation," *42nd AIAA Aerospace Sciences Meeting and Exhibit,* p. 1387, 2004.

[2] S. D. H. R. M. S. K. H. K. F. &. D. R. G. Al-Hajj, "Beirut ammonium nitrate blast: analysis, review, and recommendations', Frontiers in," pp. 9, 657996, 2021.

[3] G. agadeesh, "Industrial applications of shock waves', Proceedings of the Institution," *Part G: Journal of Aerospace Engineering 222(5),* p. 575–583, 2008.

[4] A. M. Loske, "Medical and biomedical applications of shock waves," 2017.

[5] J. Z. L. M.-Y. X. Z.-J. W. J.-P. Z. S.-j. Y. S.-b. &. W. B. Ma, "Recent progress, development trends, and consideration of continuous detonation engines," *AIAA Journal 58(12),* 2020.

[6] M. J. Chorin A.J., "Gas Flow in One Dimension. In: June M. (Eds.), A Mathematic Introduction to Fluid Mechanics," *New York : Springer-Verlag,* p. 233, 2000.

[7] G. B.-D. ‹. I. ‹. Elperin, "Shock Waves: Proceedings of the 24th International," p. 365, 2015.

[8] Y. H. ‹. M. ‹. Schmidt, "Shock Waves in Condensed Matter – 1987. 1988," p. 257, 1988.

[9] D. H. K. K. . S.K. Gupta, "Shock-tube studies of shock wave interactions with porous media," *Journal of Fluid Mechanics,* p. 175, 2016.

[10] J. S. L. G. Zhang .M.Y., "One-Dimensional Flow of Ideal Compressible Fluid. In: Xinqi L.(Eds.),Higher Engineering Fluid Mechanics.," *Xi'an Jiao tong : University Press, Xi'an,* pp. 335-361, 2006.

[11] D. H. K. K. S.K. Gupta, "Shock-tube studies of shock wave interactions with porous media," 2016.

[12] M. J. Chorin A.J., Gas Flow in One Dimension. In: June M. (Eds.), A Mathematic Introduction to Fluid Mechanics, New York: Springer-Verlag, 2000.

[13] J. S. L. G. Zhang .M.Y., One-Dimensional Flow of Ideal Compressible Fluid. In: Xinqi L.(Eds.), Higher Engineering Fluid Mechanics, Xi'an Jiao tong: University Press, Xi'an, 2006.

[14] P. Roe, "Approximate Riemann Solvers, Parameter Vectors and Difference Schemes,J. Comput. Phys. 43," pp. 357 - 372 , 1981.

[15] M. H. &. P.Garcia-Navarro, "Flux Difference Splitting and the Balancing of Source Terms and Flux Gradients, Numerical Analysis Report 3/99, University of Reading," 1999.

[16] C. M. P. R. &. B. B. Einfeldt, "Sjogreen, On Godunov-Type Methods Near Low Densities, J. Comput. Phys.," pp. 92,273-295 , 1991.

[17] P. L. &. B. V. L. A. Harten, "On Upstream Differencing and Godunov-Type Schemes for Hyperbolic Conservation Laws, SIAM Rev Vol. 25," pp. No.1, 35 -61, 1981.

[18] A. M.S. Liou, "Sequel to AUSM: AUSM+, J. Comput. Phys. 129,," pp. 364 - 382, 1996.

[19] M. H. &. P. Garcia-Navarro, "Flux Difference Splitting and the Balancing of Source Terms and Flux Gradients," *Numerical Analysis Report 3/99, University of Reading* , 1999.

[20] A. R. S. P.L. Roe, "arameter Vectors and Difference Schemes,J. Comput. Phys. 43," pp. 357 - 372, 1981.

[21] E. Toro, "Riemann Solvers and Numerical Methods for Fluid Dynamics 2nd Edn," *Springer* , 1999.

[22] C. M. P. R. &. B. S. B. Einfeldt, "On Godunov-Type Methods Near Low Densities,," *J. Comput. Phys,* pp. 92,273-295, 1991.

[23] P. L. &. B. V. L. A.Harten, "On Upstream Differencing and Godunov-Type Schemes for Hyperbolic onservation Laws," *SIAM Rev. Vol. 25 No.1,* pp. 35 -61, 1983.